UNCLASSIFIED

SECURITY CLASSIFICATION OF THIS PAGE *(When Data Entered)*

REPORT DOCUMENTATION PAGE		READ INSTRUCTIONS BEFORE COMPLETING FORM
1. REPORT NUMBER TECHNICAL REPORT ARBRL-TR-02559	2. GOVT ACCESSION NO.	3. RECIPIENT'S CATALOG NUMBER
4. TITLE *(and Subtitle)* A THEORY OF RATE-DEPENDENT PLASTICITY		5. TYPE OF REPORT & PERIOD COVERED Final Report 6. PERFORMING ORG. REPORT NUMBER
7. AUTHOR(s) WILLIAM H. DRYSDALE		8. CONTRACT OR GRANT NUMBER(s)
9. PERFORMING ORGANIZATION NAME AND ADDRESS US Army Ballistic Research Laboratory, ARDC ATTN: DRSMC-BLI(A) Aberdeen Proving Ground, MD 21005		10. PROGRAM ELEMENT, PROJECT, TASK AREA & WORK UNIT NUMBERS 1L161102AH43
11. CONTROLLING OFFICE NAME AND ADDRESS US Army AMCCOM, ARDC Ballistic Research Laboratory, ATTN: DRSMC-BLA-S(A) Aberdeen Proving Ground, MD 21005		12. REPORT DATE May 1984 13. NUMBER OF PAGES 61
14. MONITORING AGENCY NAME & ADDRESS*(if different from Controlling Office)*		15. SECURITY CLASS. *(of this report)* UNCLASSIFIED 15a. DECLASSIFICATION/DOWNGRADING SCHEDULE

16. DISTRIBUTION STATEMENT *(of this Report)*

Approved for public release; distribution unlimited.

17. DISTRIBUTION STATEMENT *(of the abstract entered in Block 20, if different from Report)*

18. SUPPLEMENTARY NOTES

19. KEY WORDS *(Continue on reverse side if necessary and identify by block number)*

Plasticity
Viscoplasticity
Rate Effects
Inelasticity
Constitutive Equations

20. ABSTRACT *(Continue on reverse side if necessary and identify by block number)* rsb, jmk

The classical theory of rate-independent plasticity is modified by the addition of a rate variable to the yield surface. From considerations of physical metallurgy it is shown that the correct parameter to add is the effective plastic strain rate. Constitutive equations suitable for a rate-dependent elastic-plastic finite element structural analysis code are derived. For the simple loading case of uniaxial stress, an exact solution is derived which models many of the rate-dependent effects observed in material testing, e.g. the behavior of the stress-strain curves for constant rate tests, change

DD FORM 1 JAN 73 1473 EDITION OF 1 NOV 65 IS OBSOLETE

(see other side of page)

UNCLASSIFIED

SECURITY CLASSIFICATION OF THIS PAGE *(When Data Entered)*

20. (continued)

of rate tests, creep/relaxation above yield, etc.

AD

TECHNICAL REPORT ARBRL-TR-02559

A THEORY OF RATE-DEPENDENT PLASTICITY

William H. Drysdale

May 1984

US ARMY ARMAMENT RESEARCH AND DEVELOPMENT CENTER
BALLISTIC RESEARCH LABORATORY
ABERDEEN PROVING GROUND, MARYLAND

Destroy this report when it is no longer needed.
Do not return it to the originator.

Additional copies of this report may be obtained from the National Technical Information Service, U. S. Department of Commerce, Springfield, Virginia 22161.

The findings in this report are not to be construed as an official Department of the Army position, unless so designated by other authorized documents.

The use of trade names or manufacturers' names in this report does not constitute indorsement of any commercial product.

TABLE OF CONTENTS

LIST OF ILLUSTRATIONS

I. INTRODUCTION

The assessment of structural integrity for bodies subjected to rapid or impulsive loading poses a severe test for the stress analyst. The difficulty arises not only from the frequent requirement for dynamic rather than static analyses but also from the deviation of the materials from classical elastic-plastic behavior under these conditions. High rates of loading lead to measurable elevation of the apparent yield strength for many structural materials. For example, the common titanium alloy, Ti 6Al - 4V, has an increase in yield stress greater than 20% due to an increase of testing strain rate from 10^{-2} to 10^{2} per second. This change represents a significant "strengthening" of the material, which should surely be included in any analysis attempting to give a complete picture of the structural response.

Extensive catalogs[1,2] and reports[3] are available which document this yield stress vs. strain rate variation for many materials of interest under constant strain rate test conditions. Unfortunately the use of these data for structural analysis is not straightforward. A few service loading histories may be approximately related to a constant strain rate. The most notable is the study of failure modes for structures rapidly loaded above their ultimate strength. An average strain rate is found by dividing the strain at failure by the duration of the phenomenon. Material properties appropriate to this rate (the "dynamic" material properties) may be used to model the failure conditions in the material, using the classical rate-independent plasticity.

More generally, the structure is intended to survive the applied forces, which consist of highly variable loading and unloading phases with possible periods of constant load interspersed. The duration of the loading phase and a maximum strain approximation may again be used to estimate strain rate for the purpose of assigning material properties. However, this rate estimate is not valid in the vicinity of the peak load, obviously the most interesting time from a structural integrity point of view. At the occurrence of maximum stress in a component, the stress rate is zero; so, the elastic strain rate is also zero. Classical plasticity theory claims that no plastic strain occurs during a neutral loading increment; therefore, the plastic strain rate is zero. Thus the total strain rate is zero at peak load, so that "static" rather then "dynamic" material properties would appear to be appropriate. The "strengthening" of many metals accompanying high rates of loading would not appear to affect the ability of a structure to survive a loading pulse. This

---

1 *U.S. Lindholm, L.M. Yeakley, R.L. Bessey, "An Investigation of the Behavior of Materials Under High Rates of Deformation," Air Force Materials Laboratory TR-68-194, Wright-Patterson AFB, OH, July 1968.*

2 *U.S. Lindholm, R.L. Bessey, "A Survey of Rate Dependent Strength Properties of Metals," Air Force Materials Laboratory TR-69-119, Wright-Patterson AFB, OH, April 1969.*

3 *A.J. Holzer, "A Tabular Summary of Some Experiments in Dynamic Plasticity," Journal of Engineering Materials and Technology, Vol. 101, pp 231 - 237, July 1979.*

simple approach cannot estimate how the stress state will be modified in passing from the high rate loading phase to the zero rate maximum stress state.

The difficulty with the preceding simple approach is due to the "grafted on" nature of the rate dependency. The rate of loading affects the incremental plastic behavior as it is occurring, and hence the state of stress and strain at peak load is dependent on this earlier load and rate history. A consistent model of the dependency of incremental plastic strain on variable loading rates is required by the stress analyst.

It is the purpose of the present work to derive such a model. The selected approach allows the retention of the elegant conceptual developments of yield surfaces, associated flow rules, normality conditions, etc., occurring in the classical rate-independent formulation. The addition of a single state variable in the description of the yield surface and the derivation of the consequences within the framework of the classical theory create a consistent theory of rate-dependent plasticity.

II. PROLEGOMENA

A. Physical Concepts

The model to be developed will be a phenomenological one; that is, it will not be deduced directly from physical considerations of crystal metallurgy. However, a brief discussion of the underlying physical processes will aid in the specification of the state parameters and concepts to appear in the theory.[4,5,6]

The division of a total differential strain increment into an elastic and a plastic part is regarded not as a computational tool but as a reflection of the physical process. Some difficulties in the definition of reference configurations for the elastic and plastic strains occur during large deformation.[7] These problems are avoided in the present work by assuming infinitesimal deformations, so that the underlying constitutive development may be emphasized. Thus

---

4 *U.F. Kocks, "Constitutive Relations for Slip," Constitutive Equations in Plasticity, ed. A.S. Argon, MIT Press, Cambridge, MA, 1975.*

5 *J.M. Kelly and P.G. Gillis, "The Influence of a Limiting Dislocation Flux on the Mechanical Response of Polycrystalline Metals," International Journal of Solids and Structures, Vol. 10, pp 45 - 59, 1974.*

6 *A.S. Argon, "Physical Basis of Constitutive Equations for Inelastic Deformation," Constitutive Equations in Plasticity, ed. A.S. Argon, MIT Press, Cambridge, MA, 1975.*

7 *E.H. Lee, "Some Comments on Elastic-Plastic Analysis," International Journal of Solids and Structures, Vol. 17, pp 859 - 872, 1981.*

$$d\varepsilon_{ij} = d\varepsilon^{e}_{ij} + d\varepsilon^{p}_{ij} \quad , \tag{1}$$

where $d\varepsilon_{ij}$ = total strain differential ,

$d\varepsilon^{e}_{ij}$ = elastic strain ,

$d\varepsilon^{p}_{ij}$ = plastic strain .

The "recoverable" or elastic strain occurs in some specific structural configuration of the crystal by the development of small increments to the distance between lattice points. It is kinematically possible for this deformation to occur instantaneously, with all lattice points displacing simultaneously. The deformations are resisted by the atomic bonds of various order, corresponding to electro-magnetic forces within the crystal, which are proportional to the lattice spacing. Specifically, they do not depend on the rate of deformation. On a continuum scale this last observation is equivalent to the rate independence of the elastic modulus for metals. Only the mass properties of the atoms in the lattice prevent the elastic strains from occurring instantaneously. The mass effect limits the propagation of elastic strain to the elastic wave speed of the material.

The "permanent" or plastic strain, on the other hand, is related to incremental changes in the structural order of the crystalline configuration by such sequential mechanisms as the movement of dislocations on glide planes. For a given level of applied force and temperature, i.e., for a given energy level in the material, dislocations move at a definite velocity determined by the average time to overcome a barrier in the glide plane. The movement of atoms due to the accumulated passing of dislocations through the crystal produces a localized plastic shear strain in the lattice.[6,8] The sequential accumulation of processes, each occurring at a finite rate, means that the plastic strain requires time to develop fully.

On the macroscopic level, the development of plastic deformation with time is apparent as a time dependency of plastic strain. This time effect has been noted by several investigators.[9,10] As stated by Phillips,[10] "To each increment of stress $d\sigma$ at a given temperature corresponds an increment of

---

8 *M.F. Ashby and H.J. Frost, "The Kinetics of Inelastic Deformation Above 0°K," Constitutive Equations in Plasticity, ed. A.S. Argon, MIT Press, Cambridge, MA, 1975.*

9 *E. Krempl, "An Experimental Study of Room-Temperature Rate-Sensitivity, Creep and Relaxation of AISI Type 304 Stainless Steel," Journal of Mechanics and Physics of Solids, Vol. 27, pp 363 - 375, 1979.*

10 *A. Phillips, "The Foundations of Plasticity," Plasticity in Structural Engineering - Fundamentals and Applications, Springer-Verlag, NY, 1979.*

elastic strain $d\varepsilon^e$ and an increment of plastic strain $d\varepsilon^p$, which needs time to develop."

This discussion of strain components shows that the plastic strain contains the rate dependency as a material response property. The elastic strain rate depends on the rate of stress application, so the elastic response to a change of stress rate is instantaneous. The time dependency of the total strain is therefore due solely to the presence of a plastic strain increment within it.

The quantity which exhibits time/rate dependency as an essential feature, conversely, is best able to serve as a rate variable in the parameterization of the macroscopic rate effects. For this reason plastic strain rate will be used as the appropriate rate variable in the present theory. The total strain rate, while it contains this parameter, also contains extraneous elastic rate data which does not reflect material response.

If the plastic strain is allowed sufficient time (perhaps infinite) to develop completely before the next stress increment is imposed, for example during a standard tensile test, the resulting plot of stress vs. total strain (elastic plus plastic) is referred to as the static stress-strain curve. For most practical loading rates, the full plastic strain will not have developed before the next stress increment is applied. The result is an apparent stiffening of the material by the suppression of a part of the time dependent plastic strain. All real stress-strain curves lie above the static curve.

Plastic deformation occurs whenever dislocations move within a crystal, even for vanishingly small stress levels.[9,11] However, the magnitude of this plastic deformation is negligible at low stress levels. Near some level of stress depending on the material, a rather abrupt transition region occurs, with the appearance of long-range movement of dislocations[4] and measurable plastic deformation. The vastly different material behavior on either side of this narrow transition region lends itself well to the concept of a unique yield or flow stress and the use of back-extrapolation techniques to determine the value.

The use of the term "plastic" strain for the permanent changes of crystal structure is widely used in Materials Science. However, it includes more than is commonly meant by the structural engineer, due to his familiarity with the classical form of plasticity theory. Not only is plastic deformation rate-dependent, but creep and relaxation effects similar to viscoelastic behavior are observed to appear above the yield stress in metals tested near room temperature.[9,10] This is, of course, a consequence of the presumption that the plastic strain increment, corresponding to a particular stress increment, needs time (perhaps infinite) to develop fully. The creep described by this mechanism is of the type commonly labeled (logarithmic) transient creep.[12]

---

[11] *S.R. Bodner and Y. Partom, "Constitutive Equations for Elastic - Viscoplastic Strain - Hardening Materials," Journal of Applied Mechanics, Vol. 42, pp 385 - 389, June 1975.*

[12] *F.A. McClintock and A.S. Argon, eds., Mechanical Behavior of Materials, Addison-Wesley Publishing Co., Reading, MA, 1966.*

Specifically it is not steady state creep which occurs in metals at elevated temperatures. To preclude this latter type of large scale deformation, which is primarily a thermally activated and controlled process, the temperature will be restricted in the present development to values less than .3 T_m (T_m is the absolute melting temperature). In this temperature range plastic deformation is dominated by the dislocation glide motion.[8,12]

Other than this restriction on the permissible temperature range, no thermal effects are considered in the present development in order to minimize the number of internal variables and, hence, to isolate the rate effect on plastic behavior. For higher temperatures, where thermally activated mechanisms become relatively more important, or for larger deformations or impact conditions, where a considerable amount of plastic work is liberated as heat, this athermal assumption becomes increasingly poor for defining material behavior.[13]

B. Phenomenological Concepts

The present development may be regarded as an extension of the classical rate-independent theory of plasticity. As such, the fundamental concepts of that theory, as described, e.g., in the books of Martin[14] and Mendelson,[15] are adopted directly.

A basic notion of the classical plasticity is the concept of stress space. Stress space is imagined as nine dimensional, each dimension corresponding to a component of stress in some reference configuration. The state of stress for every particle of a body then corresponds to a point in the stress space, and a loading and unloading process applied to the body generates a trajectory in the stress space for each particle of the body. The origin of the space is the stress-free state. It is generally assumed that there exists a neighborhood of the origin, for a virgin material, which behaves in a purely elastic manner. When the stress is increased along any stress axis, an intensity will eventually be reached such that plastic behavior occurs. This stress level corresponds to the yield stress under the particular loading program. (As remarked previously, the appearance of macroscopic plastic deformation corresponds to the development of long-range glide of dislocations. This development occurs over a rather small band of stress levels; nevertheless, the method used to determine the unique "yield stress" affects the value obtained.) By loading from a stress free state along other radial lines in the stress space until plastic deformation appears, a locus of yield stress is obtained. It is assumed that this locus

---

13 *O.W. Dillon, Jr., "Some Experiments in Thermoviscoplasticity," Constitutive Equations in Viscoplasticity: Phenomenological and Physical Aspects, AMD-Vol. 21, American Society of Mechanical Engineers, NY, 1976.*

14 *J.B. Martin, Plasticity: Fundamentals and General Results, MIT Press, Cambridge, MA, 1975.*

15 *A. Mendelson, Plasticity: Theory and Application, Macmillan Co., NY, 1968.*

forms a smooth surface in the stress space, called the initial yield surface. The surface may be analytically formulated in various ways, depending on the desired trade-off between accuracy and complexity.

When the stress point moves within the yield surface, strictly reversible strain is assumed to occur. Thus the yield surface is not altered in any way. Those portions of a load path which contact the yield surface correspond to increments of plastic strain which change the structure of the metal crystal and, hence, may be inferred to influence the yield surface. This influence is felt through the instantaneous values of a set of parameters referred to as internal variables.[14,16] The past stressing of the material in the plastic range alters the values of these parameters; in this sense, the "history" of the loading process is recorded.

The hardening behavior of the material, i.e., the change of the initial yield surface due to plastic straining, is expressed in terms of these parameters. If the initial yield surface is placed into a functional form as

$$F(\sigma_{ij}) = 0,$$

the subsequent yield surfaces following plastic strain are symbolically written as

$$F(\sigma_{ij}, \text{history}) = 0. \tag{2}$$

In a geometrical picture, when a stress point moves along a stress trajectory representing load so that it contacts the yield surface, the surface is not penetrated. Rather, the surface translates and deforms in the expanded $(\sigma_{ij}, \text{history})$ space such that the stress point and surface remain in contact. After any increment in loading corresponding to plastic deformation, the yield surface is still given by Eq. (2); thus, during plastic straining

$$dF(\sigma_{ij}, \text{history}) = 0 \ . \tag{3}$$

Note that this common assumption, in effect, defines an equation of plastic state, since the subsequent yield surfaces, Eq. (2), are relations among the stress and some complete set of internal variables sufficient to describe the process of plastic deformation.

The selection of the set of internal variables to describe the plastic deformation depends on the formulation of classical plasticity adopted. Some

---

16 *J.R. Rice, "On the Structure of Stress-Strain Relations for Time-Dependent Plastic Deformation in Metals," Journal of Applied Mechanics, Vol. 37, pp 728 - 737, September 1970.*

measure of change of structure in the metal crystal is required, e.g., effective plastic strain or plastic work. Also, for a rate-dependent theory to result, some form of strain-rate variable must appear in the expression for yield surface.[17] Here the selection of an internal variable is nowhere near as standard. Attempts at a theory of crystal microplasticity use a variety of parameters, such as mobile dislocation density and velocity, all of which are eventually related in some manner to the plastic strain rate.

A final concept from the classical theory of plasticity is a flow rule, i.e., a specification of the amount and relative directions of the incremental plastic strain components due to an increment of stress. The plastic strain increments must be perpendicular to the yield surface in the stress space in order to ensure material stability and uniqueness of solutions.[14] This requirement is expressed formally as

$$d\varepsilon^{P}_{ij} = d\lambda \frac{\partial F}{\partial \sigma_{ij}} , \qquad (4)$$

where $d\lambda$ = parameter expressing magnitude of plastic strain increments,

$\frac{\partial F}{\partial \sigma_{ij}}$ = normal to the yield surface $F = 0$ in the stress space.

The addition of other parameters to the specification of the yield surface, in effect increasing the dimension of the space on which subsequent yield surfaces are defined, does not eliminate this requirement for normality of the plastic strain increments in the stress subspace. Hence, the yield surface is also regarded as a potential function for plastic deformation. This associated flow rule, common to most plasticity formulations, is carried over directly to the rate-dependent case. It is expected that a number of theorems relating to stability, uniqueness, and bounds of solutions for plastic deformation, depending on the normality condition of the classical theory, would also apply then to the rate-dependent formulation.

C. Experimental Basis for Rate-Dependent Yield Stress

The type of material behavior to be modeled has been described by several investigators: Lindholm for a variety of structural materials,[1] Krempl for AISI Type 304 Stainless Steel,[9] Kujawski and Krempl for a titanium alloy,[18] etc. Typically, the data were determined from a series of constant strain

---

17 *W. Olszak, "Generalized Yield Criteria for Advanced Models of Material Response," Plasticity in Structural Engineering Fundamentals and Applications, Springer-Verlag, NY, 1979.*

18 *D. Kujawski and E. Krempl, "The Rate (Time) - Dependent Behavior of Ti-7Al-2Cb-1 Ta Titanium Alloy at Room Temperature Under Quasistatic Monotonic and Cyclic Loading," Journal of Applied Mechanics, Vol 48, pp 55-63, March 1981.*

rate uniaxial tests performed for a wide range of loading rates. An example from Reference (1) is shown as Figure 1. Common features of the plots include a unique elastic line common to all levels of strain rate. Then, for each constant strain rate test, a separate leg of the $\sigma - \varepsilon$ curve is obtained. The legs of the curve are ordered as shown, with higher applied strain rates corresponding to higher stress levels.

Another feature of the typical plot is that the legs of the curve for the different strain rates are often roughly parallel, at least for moderate strain rates below 10^3 in/in/sec. (For higher rates, thermodynamic coupling considerations would become increasingly more important.) We assume that the legs are parallel for different constant strain rates, so that the determination of the tangent modulus for static loading rates may be applied for all constant strain rates.

The investigations of rate effect are commonly performed at a constant total strain rate. As indicated previously, the preferred rate variable for the present investigation is the plastic strain rate. To convert the mass of experimental data at constant total strain rate to usable form, we further assume that the plastic strain rate approaches a constant value within a short distance along the leg of the plastic portion of the stress-strain curve. This assumption will be well justified by the results of the uniaxial test model presented in a later section.

Since the constant plastic strain rates are asymptotically approached along the plastic leg of the stress-strain curve, it is obvious that the yield stress should be obtained by a back-extrapolation along each leg. An optimum method of performing this back-extrapolation relies on the use of a bilinear stress-strain relation within the strain range of interest; the procedure is described in detail in Reference (19). The bilinear stress-strain approximation gives an easy-to-use, reasonably accurate model of elastic-plastic behavior.[19] The use of a more accurate curve is probably not justified, especially since the same curve must be fit to each of the roughly parallel plastic legs.

A bilinear representation of a stress-strain curve is shown in Figure 2. For an increment of stress $\Delta\sigma$ within the plastic range, there is an increment of elastic and plastic strain. The relation between the constant total strain rate and the assumed constant plastic strain rate given by a bilinear representation is

$$\frac{\dot{\varepsilon}^P}{\dot{\varepsilon}} = \frac{\dot{\varepsilon} - \dot{\varepsilon}^e}{\dot{\varepsilon}} = \frac{\frac{\dot{\sigma}}{E_T} - \frac{\dot{\sigma}}{E}}{\frac{\dot{\sigma}}{E_T}} = \frac{E - E_T}{E} \quad . \tag{5}$$

Eq. (5) may be used to generate data points of yield stress vs. plastic strain rate from the constant strain rate stress-strain curves shown in Figure 1. Typical results from this process are shown in Figure 3. Many similar

---

19 *C.E. Pugh, J.M. Corum, K.C. Lin and W.L. Greenstreet, "Currently Recommended Constitutive Equations for Inelastic Design Analysis of FFTF Components," ORNL-TM-3602, Oak Ridge National Lab., TN, September 1972.*

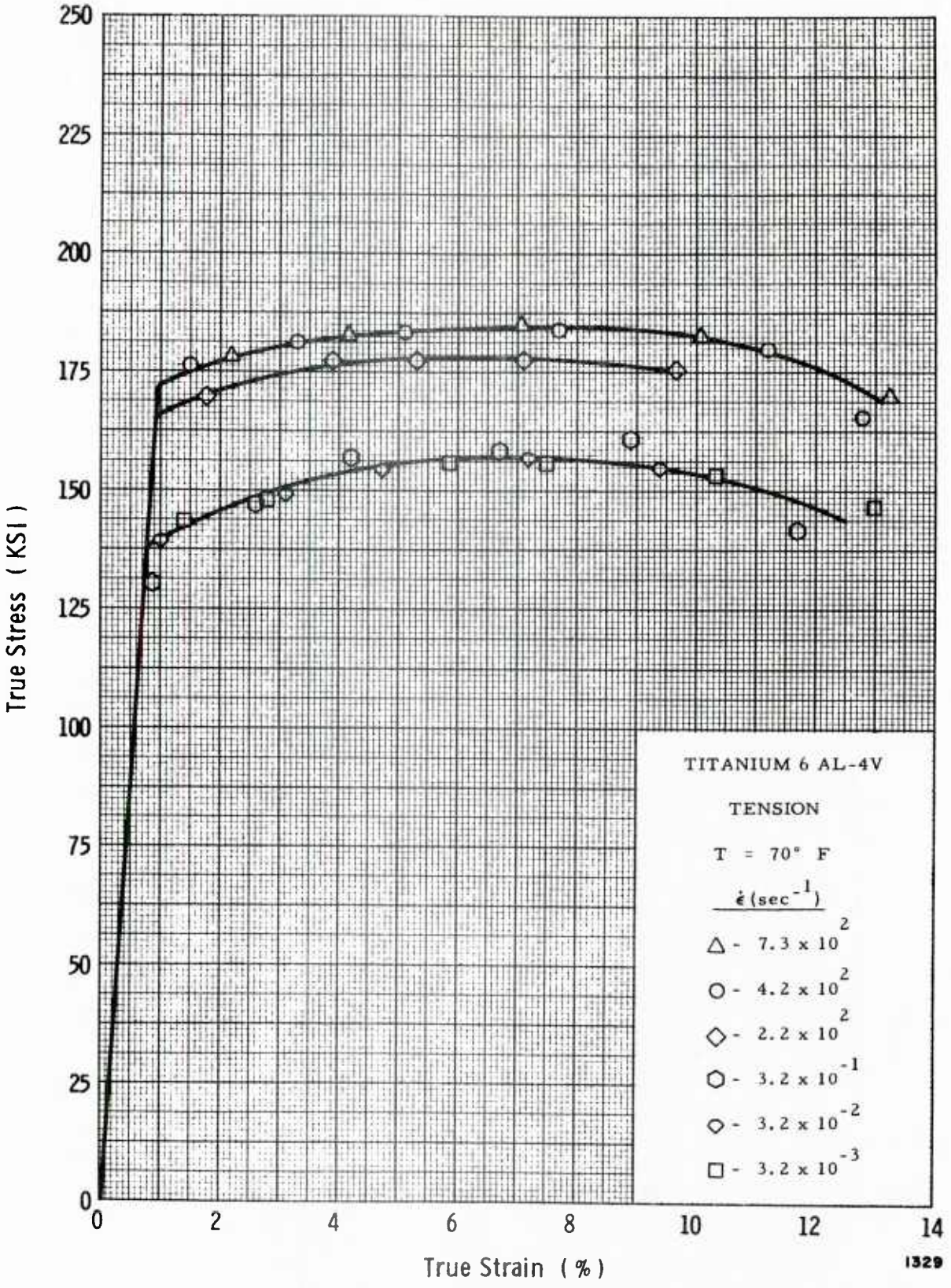

Figure 1. Typical Experimentally Determined Stress-Strain Curves Demonstrating Rate-Dependent Yield Stress (Reference 1)

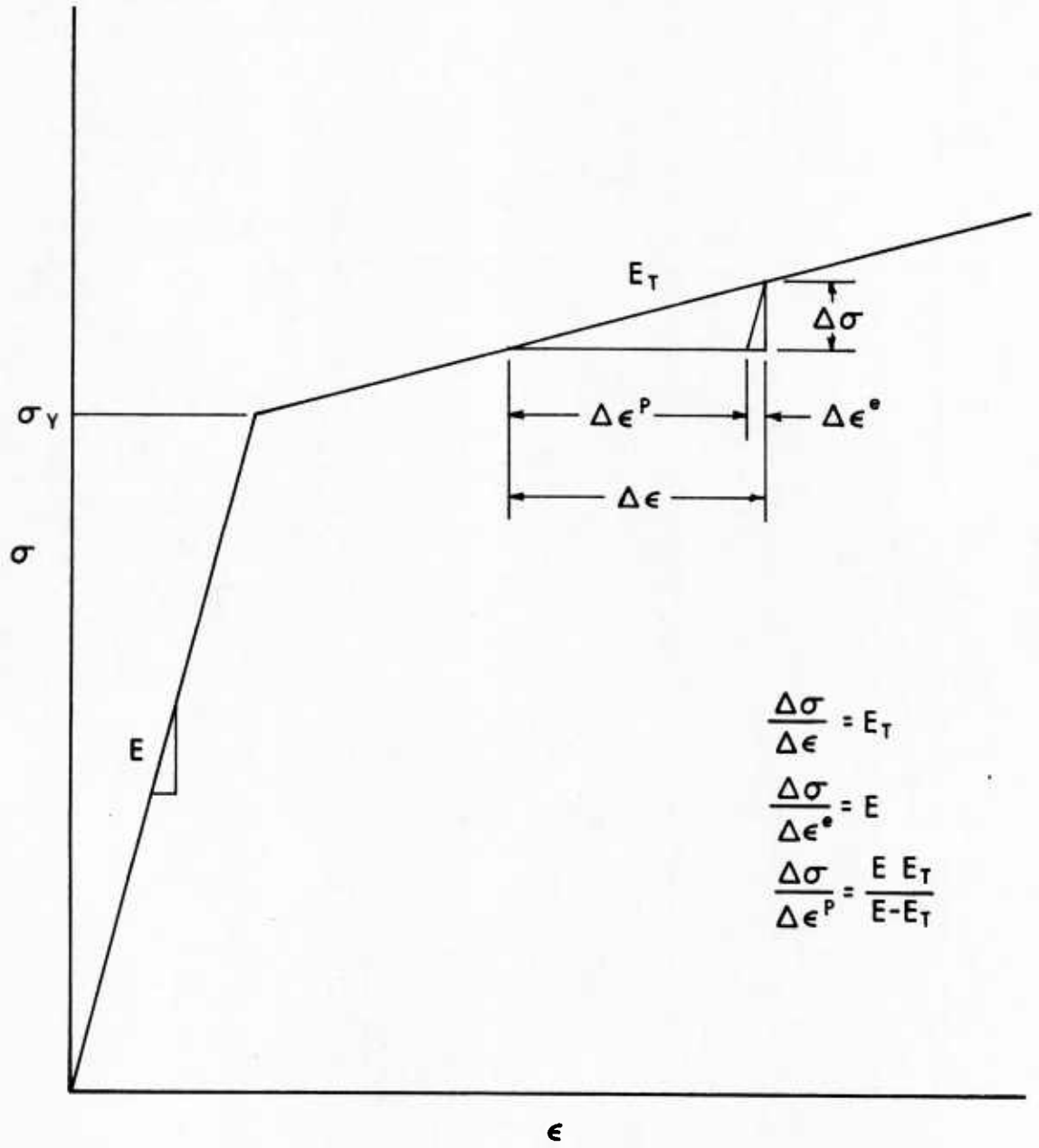

Figure 2. Bilinear Model of Uniaxial Material Test, Showing Elastic and Tangent Modulus

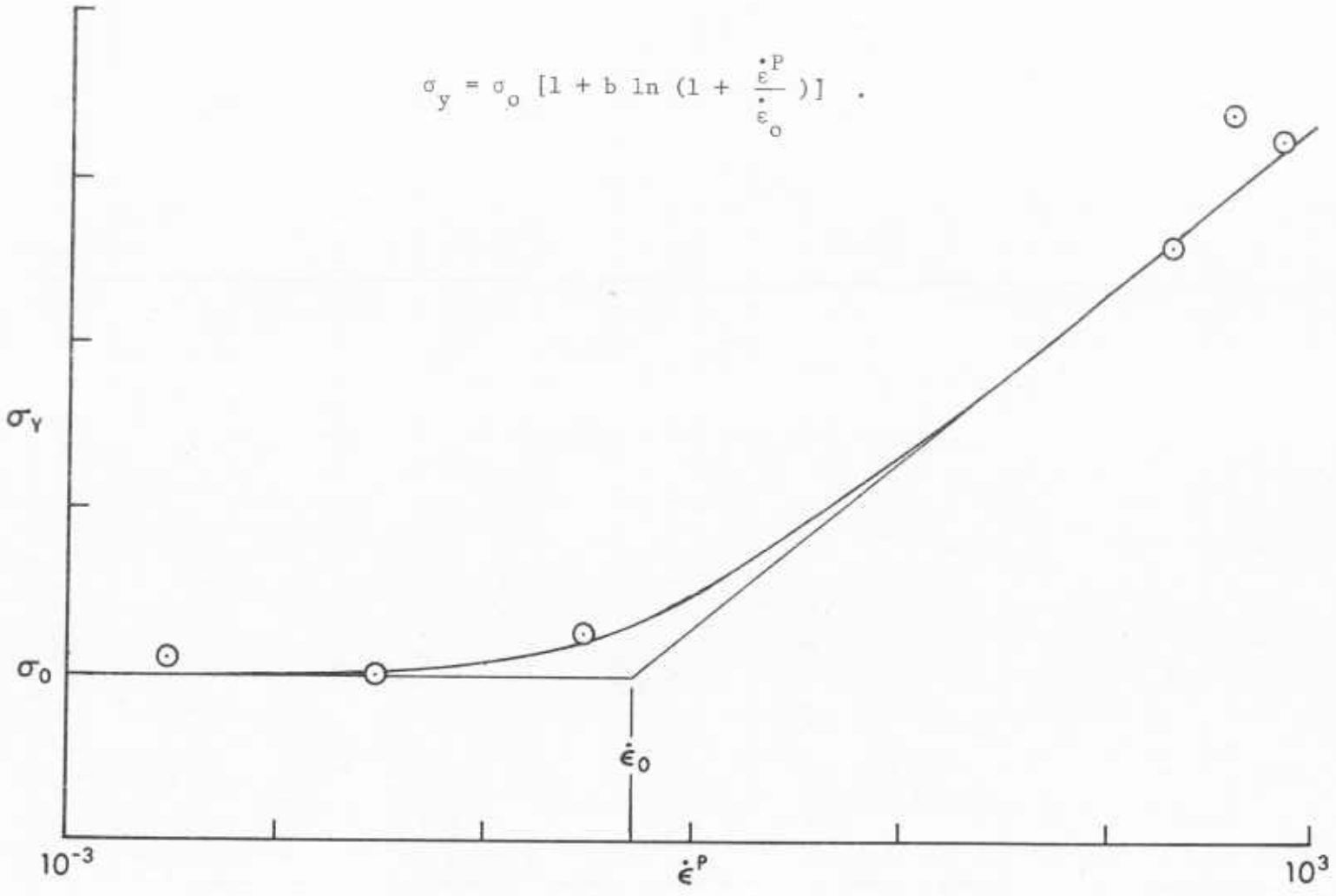

Figure 3. Typical Variation of Yield Stress with Plastic Strain Rate for Moderate Rates

plots may be seen in Reference (2), where, however, the coordinate is total strain rate, so that the scale should be adjusted by Eq. (5). Some features are common to many materials. At low rates the yield stress is nearly constant at the "static" value. Then, there exists a knee in the curve at some transition strain rate, $\dot{\varepsilon}_o$, above which the yield stress rises with plastic strain rate. This increase may be represented by a straight line on the semi-log plot, at least to within the accuracy implied by the typical large amount of scatter. The mathematical form which expresses this behavior is given by

$$\sigma_y = \sigma_o \left[1 + b \, \ell n \left(1 + \frac{\dot{\varepsilon}^P}{\dot{\varepsilon}_o}\right)\right] . \qquad (6)$$

This expression gives the yield stress σ_y in terms of the static yield stress σ_o, a slope parameter b, a plastic strain rate $\dot{\varepsilon}^P$, and a transition strain rate $\dot{\varepsilon}_o$. At very high strain rates, greater than 10^3, there appears to be a second transition, into a zone of greater strain rate sensitivity. Here the dependence is nearly linear rather then logarithmic. In Material Science it is generally presumed that a different mechanism of resistance to dislocation motion has become predominant at these higher rates, yielding the different response. In any case, these rates correspond to high speed impact problems and are not generally encountered in structural integrity analyses.

Some final observations concerning tests of material at constant strain rate deal with modifications to these tests. Thus, the rate may be suddenly changed from one rate to another higher rate. Immediately after the change of rate, the slope of the stress-strain curve is nearly elastic. The curve rapidly approaches that appropriate to a constant rate test at the higher rate; the curve soon becomes indistinguishable from a test performed entirely at the higher rate.

When a test at constant rate is interrupted in the plastic range by holding the stress or strain constant, creep or relaxation will occur in metals at room temperature. If the constant rate is reapplied to the test specimen, the stress-strain curve will rapidly approach a curve appropriate to an uninterrupted test. These last effects are well documented in the series of papers by Krempl, et al.[9, 18]

III. THEORY OF RATE-DEPENDENT PLASTICITY

A. General Formulation

Rate dependency may be added to any of the currently utilized classical theories of plasticity by the addition of an appropriate rate variable to the yield surface.[17] The resulting formulation will exhibit the defects of the underlying classical formulations. For example, a model based on isotropic strain hardening will not be able to describe cyclic loading with accuracy. Conversely, the inclusion of excessive generality in the basic theory will yield constitutive relations which are difficult to apply in practical analysis, even with the aid of advanced computers.

The present development will adopt the classical plasticity model selected in Reference (19), where a critical evaluation of currently utilized

formulations is given. Briefly, the selected model consists of a Von Mises yield criterion, with kinematic hardening, an associated incremental flow rule, and a bilinear material representation. These assumptions were chosen because of their ability to model rather general loading programs, including cyclic loading with Bauschinger effect. In addition, the resulting incremental constitutive equations are conceptually simple and easily included in nonlinear finite element structural codes, e.g., ADINA.[20] While the general development of the rate-dependent theory will be presented within this context, extension of other variants of the classical theory is straightforward.

The rate variable used in the present formulation is plastic strain rate. The reason for this selection was discussed in Section II.A, where the finite velocity of dislocation motion was judged responsible for the noninstantaneous time-dependent growth of elastic-plastic strain. The use of this rate variable in the theories of viscoplasticity, as expounded, e.g., by Perzyna,[21, 22] is based on the same type of consideration.

For consideration of the experimental results of uniaxial material tests, the uniaxial plastic strain rate is an acceptable variable. This may be generalized to multiaxial states of stress by assuming that the plastic strain rate tensor is the controlling variable, $\dot{\varepsilon}^{P}_{ij}$. However, a more coherent theory results from the further consideration of the selection of plastic strain rate as a rate variable. Since dislocation motion is the phenomenon which controls the rate of plastic deformation and the combined movement on several slip planes adds together to give each tensorial component of plastic strain rate, the total amount of dislocation motion on all active slip planes is seen as regulating the rate of plastic flow. An estimate of this combined dislocation motion appropriate to a phenomenological theory is based on "effective" plastic strain[15]. This quantity is defined in terms of increments of components of plastic strain as

$$d\varepsilon^{P} = \sqrt{2/3 \; d\varepsilon^{P}_{ij} \; d\varepsilon^{P}_{ij}} \quad \text{(summation on repeated indices)} \qquad (7)$$

The rate quantity is obtained by dividing by dt. As may be seen, effective plastic strain rate sums plastic strain rate over all components of the tensor, and may therefore serve as a measure of total "plastic activity." For the important case of uniaxial stress states as occur in material testing, the effective plastic strain rate reduces to the axial plastic strain rate, due to the incompressibility of plastic deformation.

---

20 *K.J. Bathe, "Static and Dynamic Geometric and Material Nonlinear Analysis Using ADINA," Report 82448-2, Mass. Inst. of Tech., Cambridge, MA, May 1977.*

21 *P. Perzyna, "Fundamental Problems in Viscoplasticity," Advances in Applied Mechanics, ed. by G. Kuerti, Academic Press, NY, 1966.*

22 *P. Perzyna, "Thermodynamics of Dissipative Materials," Recent Developments in Thermomechanics of Solids, Springer-Verlag, NY, 1980.*

The yield surface given by Eq. (2) may now be specified for the assumed classical plasticity model. Thus, the region of elastic behavior is bounded by

$$F(\sigma_{ij}, \varepsilon^P_{ij}, \dot{\varepsilon}^P) = f(S_{ij} - \alpha_{ij}) - K(\dot{\varepsilon}^P) = 0 \quad , \tag{8}$$

where

S_{ij} = stress deviator = $\sigma_{ij} - \sigma\ \delta_{ij}$, $\sigma = \frac{1}{3}(\sigma_{11} + \sigma_{22} + \sigma_{33})$,

$d\alpha_{ij} = C\ d\varepsilon^P_{ij}$ (kinematic hardening) ,

C = hardening modulus (constant for bilinear material) ,

$f(S_{ij} - \alpha_{ij}) = \frac{1}{2}(S_{ij} - \alpha_{ij})(S_{ij} - \alpha_{ij})$ (Von Mises form) ,

$K(\dot{\varepsilon}^P) = \frac{1}{3}\ \sigma_y^2(\dot{\varepsilon}^P)$ (magnitude of yield stress).

Any strain hardening that occurs in the kinematic model is contained in the parameter α_{ij}, which is essentially a shift of the origin of the yield surface in stress space in the direction of the plastic strain increment. (Care is required when using kinematic hardening in reduced stress spaces.)[14] Translation of the yield surface in the direction of prior plastic strain models the Bauschinger effect, as it occurs during reversed loading, with sufficient accuracy for most engineering purposes.

The hardening modulus appearing in Eq. (8) may be determined by applying that equation to a uniaxial material test. Since a bilinear model is assumed in the present analysis, as shown in Figure 2, C is constant and given by

$$C = \frac{2}{3}\ \frac{EE_T}{E-E_T} \tag{9}$$

Study of Eq. (8) reveals an additional advantage of the kinematic hardening formulation for rate-dependent plasticity, viz. the rate effect has been isolated in the term K, corresponding to yield stress. The variation of other quantities in Eq. (8) with rate of deformation is not assumed because of the lack of experimental evidence. For example, allowing E_T and, hence, C to

vary with $\dot{\varepsilon}^P$ contradicts the observed parallelism of the legs of constant rate stress-strain curves at different rates (Recall Figure 1).

Throughout a load increment which corresponds to plastic deformation, Eq. (8) must hold. Hence, the increment of F must vanish, as specified by Eq. (3). For the present formulation, this requirement becomes

$$dF = \frac{\partial f}{\partial \sigma_{ij}} d\sigma_{ij} + \frac{\partial f}{\partial \alpha_{ij}} d\alpha_{ij} - \frac{\partial K}{\partial \dot{\varepsilon}^P} d\dot{\varepsilon}^P = 0 \quad , \tag{10}$$

where

$$\frac{\partial f}{\partial \sigma_{ij}} = \frac{\partial f}{\partial S_{ij}} \quad ,$$

$$\frac{\partial f}{\partial \alpha_{ij}} = - \frac{\partial f}{\partial \sigma_{ij}} \quad .$$

With the aid of the definitions of Eq. (8), Eq. (10) becomes

$$\frac{\partial f}{\partial \sigma_{ij}} d\sigma_{ij} - C \frac{\partial f}{\partial \sigma_{ij}} d\varepsilon^P_{ij} - \frac{\partial K}{\partial \dot{\varepsilon}^P} d\dot{\varepsilon}^P = 0 \quad . \tag{11}$$

Eq. (11) connects the increments of stress, $d\sigma_{ij}$, plastic strain, $d\varepsilon^P_{ij}$, and effective plastic strain rate $d\dot{\varepsilon}^P$ and forms, in effect, an evolutionary equation for the components of plastic strain. Since it is summed over all components of stress and plastic strain, the expression governs only the magnitude of the plastic strain. To obtain the direction of the plastic strain increment an additional relation is required; this relation is the associated flow rule as expressed by Eq. (4); for the present formulation

$$d\varepsilon^P_{ij} = d\lambda \frac{\partial f}{\partial \sigma_{ij}} \quad . \tag{12}$$

The nomenclature of Eq. (12) is standard; but for the present development, an alternate form of the associated flow rule is preferred. Substituting Eq. (12) into Eq. (7) gives

$$d\varepsilon^P = \sqrt{2/3\ (d\lambda)^2 \frac{\partial f}{\partial \sigma_{ij}} \frac{\partial f}{\partial \sigma_{ij}}}$$

$$= \sqrt{2/3\ (d\lambda)^2\ 2/3\ \sigma_y^{\,2}}$$

$$= 2/3\ \sigma_y\ d\lambda\ . \tag{13}$$

Then

$$d\varepsilon^P_{ij} = 3/2\ \frac{d\varepsilon^P}{\sigma_y} \frac{\partial f}{\partial \sigma_{ij}}\ . \tag{12a}$$

Inserting Eq. (12a) into Eq. (11)

$$\frac{\partial f}{\partial \sigma_{ij}}\ d\sigma_{ij} - C\ \sigma_y\ d\varepsilon^P - 2/3\ \sigma_y \frac{\partial \sigma_y}{\partial \dot{\varepsilon}^P}\ d\dot{\varepsilon}^P = 0\ , \tag{11a}$$

and solving this expression for $d\varepsilon^P$

$$d\varepsilon^P = \frac{1}{C\sigma_y} \left[\frac{\partial f}{\partial \sigma_{ij}}\ d\sigma_{ij} - 2/3\ \sigma_y \frac{\partial \sigma_y}{\partial \dot{e}^P}\ d\dot{e}^P \right]\ . \tag{14}$$

Finally substituting this relation back into Eq. (12a)

$$d\varepsilon^P_{ij} = 3/2\ \frac{1}{C\sigma_y^{\,2}} \left[\frac{\partial f}{\partial \sigma_{k\ell}}\ d\sigma_{k\ell} - 2/3\ \sigma_y \frac{\partial \sigma_y}{\partial \dot{\varepsilon}^P}\ d\dot{\varepsilon}^P \right] \frac{\partial f}{\partial \sigma_{ij}}\ . \tag{15}$$

Eq. (15) is a constitutive relation for the increment of the plastic strain tensor, $d\varepsilon^P_{ij}$, in terms of the material properties, the normal to the yield surface, the increment of stress and an increment of effective plastic strain rate. The first term in brackets in Eq. (15) is the rate-independent equation from classical plasticity. The second term constitutes the correction for rate effect.

A form of the general equations dealing with increments of stress and total strain may be more convenient for numerical applications. The elasticity relation is

$$d\sigma_{ij} = E_{ijk\ell}\ d\varepsilon^{e}_{k\ell} = E_{ijk\ell}\ [d\varepsilon_{k\ell} - d\varepsilon^{P}{}_{k\ell}] \ . \tag{16}$$

Replacing $d\sigma_{ij}$ in Eq. (11a) by this expression and again solving for effective plastic strain increment gives

$$d\varepsilon^{P} = [\frac{\partial f}{\partial \sigma_{ij}}\ E_{ijk\ell}\ d\varepsilon_{k\ell} - 2/3\ \sigma_y\ \frac{\partial \sigma_y}{\partial \varepsilon^{\bullet P}}\ d\varepsilon^{\bullet P}]2/3\ \sigma_y\ D \ , \tag{17}$$

where

$$D = [\frac{2}{3}\ \sigma_y{}^2\ C + \frac{\partial f}{\partial \sigma_{ij}}\ E_{ijk\ell}\ \frac{\partial f}{\partial \sigma_{k\ell}}]^{-1} \ .$$

Then, using Eq. (17) and Eq. (12a) in Eq. (16) gives a modified constitutive relation

$$d\sigma_{ij} = [E_{ijk\ell} - D\ E_{ijmn}\ \frac{\partial f}{\partial \sigma_{mn}}\ \frac{\partial f}{\partial \sigma_{rs}}\ E_{rsk\ell}]d\varepsilon_{k\ell} - D\ E_{ijk\ell}\ \frac{\partial f}{\partial \sigma_{k\ell}}\ 2/3\ \sigma_y\ \frac{\partial \sigma_y}{\partial \varepsilon^{\bullet P}}\ d\varepsilon^{\bullet P} \ . \tag{18}$$

Again the rate effect is isolated in the last term. The remainder of the Eq. (18) is identical to the classical rate-independent relation.

In the present form, of course, the increment of effective plastic strain rate is unknown, so Eqs. (15) or (18) are not directly useful as computational tools without some algorithm to calculate $d\varepsilon^{\bullet P}$ for the increment. No such specification will be made for the general case; however, several solutions for special cases will be developed to cover many situations of practical interest in the following sections. Of particular importance within the context of modern engineering practice, an incremental form of the theory readily adaptable to nonlinear, dynamic, finite element stress analysis codes is a preferred embodiment and will be developed next.

B. Incremental Constitutive Relation for Computation of Multiaxial Plastic Strain

In the general development of the preceding section, the increments of the plastic strain tensor, Eq. (15), were specified by increments of stress and effective plastic strain rate, with coefficients to these increments depending on the instantaneous value of the stress and plastic strain tensor and the effective plastic strain rate. This form of the theory leaves the analyst with the problem of computing, or at least estimating, the increment of effective plastic strain rate. The correct increment will maintain the collection of state variables on the yield surface during plastic deformation and also maintain the appropriate relation between increments of tensorial plastic strain and strain rate and the effective plastic strain rate considered as time differential.

An alternate approach is obtained by returning to the expression for the vanishing of the increment of yield surface, dF, as given by Eq. (11a). Dividing this relation by dt, the corresponding increment of time, gives

$$\frac{\partial \sigma_y}{\partial \dot{\varepsilon}^P} \ddot{\varepsilon}^P + 3/2\, C\, \dot{\varepsilon}^P = 3/2 \left(\frac{1}{\sigma_y} \frac{\partial f}{\partial \sigma_{ij}}\right) \dot{\sigma}_{ij} \quad , \tag{19}$$

where

$\ddot{\varepsilon}^P$ = effective plastic strain "acceleration."

This equation will be considered a first-order nonlinear differential equation for the plastic strain rate. The nonlinearity arises from the coefficients of the equation.

The empirical relation Eq. (6) for the variation of yield stress with plastic strain rate may be differentiated to give

$$\frac{\partial \sigma_y}{\partial \dot{\varepsilon}^P} = \frac{\sigma_o b}{\dot{\varepsilon}_o + \dot{\varepsilon}^P} \quad . \tag{20}$$

This is the coefficient of the acceleration term.

The right hand side of Eq. (19) presents a greater difficulty. The quantity in parentheses represents the direction normal to the yield surface in stress space, assumed to be the direction of the incremental plastic flow by the associated flow rule. The magnitude of this gradient to the yield surface has been normalized by dividing by σ_y. Hence this quantity represents a vector of constant magnitude but variable direction in the stress space. The scalar product of this normal with the stress rate vector constitutes the

loading associated with the plastic deformation; this concept is directly from the classical theory. The analytical specification of this normal direction generates enormous difficulties in the general case, although the form is simple,

$$\frac{1}{\sigma_y}\frac{\partial f}{\partial \sigma_{ij}} = \frac{(S_{ij} - C\,\varepsilon^P_{ij})}{\sqrt{3/2\ (S_{k\ell} - C\varepsilon^P_{k\ell})(S_{k\ell} - C\varepsilon^P_{k\ell})}} \quad . \tag{21}$$

The real difficulty arises from the mere appearance of the individual components of the plastic strain tensor. Eq. (19) may no longer be considered a nonlinear differential equation; its true character as a nonlinear integro-differential equation becomes apparent due to the requirements of specifying the plastic strain tensor.

The difficulties with the right hand side of Eq. (19) disappear in two special cases, which have also been widely investigated in classical plasticity. The first is the case of perfect plasticity. In this approximation there is no work or strain hardening during plastic deformation; i.e., the tangent modulus in the plastic state is assumed to be zero, which gives $C = 0$ in the present formulation. The true significance of this model, however, lies in the fact that the yield surface, and hence the normal to the yield surface, no longer depends in any way on the plastic strain which has occurred up to that time.

The second special case concerns restricted loading programs, in particular what is commonly called radial or proportional loading. In this case the load in stress space proceeds along a radius of the yield surface until that surface is reached. Additional loads are applied in the same direction in the stress space, i.e., the relative proportions of the various components of the stress tensor are maintained constant throughout the plastic deformation. The initial normal to the yield surface is given by Eq. (21) with $\varepsilon^P_{ij} = 0$, so the initial increments of plastic strain are also in this radial direction. Thus, no changes in the direction of the normal occur during proportional loading; and the coefficient on the right hand side becomes constant.

These two solutions to the difficulties presented by Eq. (19) rely on special material or loading assumptions. Hence they are not applicable to general structural analysis. The remainder of the current section will develop an approximate method appropriate to the numerical structural analysis of general material properties and loading programs. The method commonly applied to compute nonlinear behavior by modern structural analysis codes (e.g., Reference (20)) is to replace the differential (infinitesimal) increment developed in the preceding sections to describe the growth of the plastic strain by a finite increment or difference. During the finite increment, only the incremental quantities grow; all other quantities (e.g., stress, plastic strain, etc.) remain fixed at the values at the beginning of

the increments. At the beginning of the next increment, these total quantities are adjusted by the value of the preceding increment. Hence the total quantities vary as step functions. This type of approximation is accurate as the duration of the increment approaches zero. For finite intervals the accuracy may be improved by decreasing the size of the increment or by iterating the value of the total functions within the interval. The rationale for this procedure comes from the mean value theorem of elementary calculus.

Applying this procedure in the present case means that the coefficients and right hand side of Eq. (9) are constant. Hence the equation reduces to a linear, first-order differential equation for $\dot{\varepsilon}^P$, which is readily solvable within each of the finite intervals. The incremental time scale will be denoted by τ; the origin is placed at the beginning of each increment.

The complementary solution of Eq. (19) is

$$\dot{\varepsilon}^P = \beta \exp \left[- \frac{3/2\ C}{\dfrac{\partial \sigma_y}{\partial \dot{\varepsilon}^P}} \tau \right] , \tag{22}$$

where β = constant of integration.

The complete solution of Eq. (19) is obtained by variation of parameters. β in Eq. (22) is assumed to be no longer constant, but rather a function of τ. Inserting Eq. (22) into Eq. (19) gives

$$\dot{\beta} = 3/2 \left(\frac{1}{\sigma_y} \frac{\partial f}{\partial \sigma_{ij}} \right) \dot{\sigma}_{ij} \frac{1}{\dfrac{\partial \sigma_y}{\partial \dot{\varepsilon}^P}} \exp \left[\frac{3/2\ C\ \tau}{\dfrac{\partial \sigma_y}{\partial \dot{\varepsilon}^P}} \right] , \tag{23}$$

which may be integrated to give

$$\beta = \left(\frac{1}{\sigma_y} \frac{\partial f}{\partial \sigma_{ij}} \right) \frac{\dot{\sigma}_{ij}}{C} \exp \left[\frac{3/2\ C\ \tau}{\dfrac{\partial \sigma_y}{\partial \dot{\varepsilon}^P}} \right] + \beta_1 , \tag{24}$$

where β_1 = constant of integration.

Substituting Eq. (24) into Eq. (22) gives the complete solution

$$\dot{\varepsilon}^P = \frac{1}{C}\left(\frac{1}{\sigma_y}\frac{\partial f}{\partial \sigma_{ij}}\right)\dot{\sigma}_{ij} + \beta_1 \exp\left[-\frac{3/2\ C\ \tau}{\frac{\partial \sigma_y}{\partial \dot{\varepsilon}^P}}\right] . \qquad (25)$$

To evaluate the constant, β_1, the discussion of previous sections will be recalled. There, it was postulated that the resistance of the plastic strain rate (caused by dislocation motion) to sudden changes was the basis of the rate effect in plastic deformation. Hence, the correct initial condition for Eq. (25) is to guarantee continuity of the effective plastic strain rate from the previous increment.

$$\dot{\varepsilon}^P = \dot{\varepsilon}^P_o , \quad \text{when } \tau = 0 . \qquad (26)$$

Thus

$$\beta_1 = \dot{\varepsilon}^P_o - \frac{1}{C\sigma_y}\frac{\partial f}{\partial \sigma_{ij}}\dot{\sigma}_{ij} . \qquad (27)$$

Eq. (25) must be converted from an expression for effective plastic strain rate to a relation for the increment of effective plastic strain for use in the associated flow rule Eq. (12a). The increments are now finite rather than differential, so

$$d\varepsilon^P = \dot{\varepsilon}^P \tau$$

and (28)

$$d\sigma_{ij} = \dot{\sigma}_{ij} \tau .$$

Collecting Eqs. (12a), (25), (27) and (28) generates a constitutive equation for the increment of plastic strain

$$d\varepsilon^{P}_{ij} = 3/2 \frac{1}{C\sigma_y^2} \frac{\partial f}{\partial \sigma_{k\ell}} d\sigma_{k\ell} \frac{\partial f}{\partial \sigma_{ij}}$$

$$+ 3/2 \frac{\tau}{\sigma_y} \left(\dot{\varepsilon}^{P}_{o} - \frac{1}{C\sigma_y} \frac{\partial f}{\partial \sigma_{k\ell}} \dot{\sigma}_{k\ell}\right) \exp\left[- \frac{3/2\ C\ \tau}{\frac{\partial \sigma_y}{\partial \varepsilon^{P}}}\right] \frac{\partial f}{\partial \sigma_{ij}} . \qquad (29)$$

The first term on the right hand side of Eq. (29) is the classical rate-independent plastic increment. The second term represents the correction for rate effect. It controls the growth of the plastic strain increment with time within the interval and demonstrates the continuous evolution of plastic strain with time as postulated from physical considerations; even for constant stress, when

$$d\sigma_{k\ell} = \dot{\sigma}_{k\ell} = 0 .$$

Eq. (29) shows that plastic strain will grow due to the initial effective plastic strain rate in the interval. This phenomenon is creep occurring above the yield strength of the material.[9,10]

The form of Eq. (29) is well suited for use in incremental elastic-plastic finite element codes.[23] The structure of the code does not need to be changed, since all quantities required to calculate the plastic deformation during an increment are available at the beginning of the increment. Additional algebraic operations are, of course, required in each increment to obtain the correction for rate effect.

C. Development for Perfectly Plastic Material

For a perfectly plastic material there is no strain hardening. In the development for the classical theory the stress may not increase beyond the (static) yield surface. In the rate dependent theory, some increase of stress above static yield is possible due to rate hardening of the material. The significance of the perfectly plastic model lies in the immense simplification of the yield surface definition possible without hardening. The difficulty introduced in the general case by a yield surface dependent on the integrated past history of plastic deformation was considered in the discussion following Eq. (19).

In the present formulation, the perfectly plastic model is obtained by eliminating the kinematic hardening, i.e., C = 0. Then Eq. (11) becomes

---

[23] *A.R. Zak, "Finite Element Model for Nonaxisymmetric Structure with Rate Dependent Yield Conditions," BRL Contractor Report, In preparation.*

$$\frac{\partial f}{\partial \sigma_{ij}} \, d\sigma_{ij} = \frac{\partial K}{\partial \dot{\varepsilon}^{P}} \, d\dot{\varepsilon}^{P} \quad , \tag{30}$$

which is integrable, giving the original yield function. Thus

$$1/2 \, S_{ij} \, S_{ij} = \frac{\sigma_o^2}{3} \left[1 + b \, \ell n \left(1 + \frac{\dot{\varepsilon}^{P}}{\dot{\varepsilon}_o}\right)\right]^2 . \tag{31}$$

Solving for effective plastic strain rate

$$\dot{\varepsilon}^{P} = \dot{\varepsilon}_o < \exp \left[\frac{\sqrt{3/2 \, S_{ij} S_{ij}} - \sigma_o}{b \, \sigma_o}\right] - 1 > \quad , \tag{32}$$

from which a rate form (the traditional form) for components of plastic strain results, giving

$$\dot{\varepsilon}^{P}_{ij} = \frac{3}{2} \, \dot{\varepsilon}_o < \exp \left[\frac{\sqrt{3/2 \, S_{ij} S_{ij}} - \sigma_o}{b\sigma_o}\right] - 1 > \frac{S_{ij}}{\sigma_y} . \tag{33}$$

The plastic strain rate may be seen in Eq. (33) to be in the direction of the current value of the stress deviator tensor, and of a magnitude influenced by an exponential function of the excess of "effective stress" over the static yield stress. For a constant stress condition, the plastic flow will continue indefinitely.

D. Model of Uniaxial Stress States

The incremental solution indicated in Section B allows general loading programs to be numerically modeled with any required accuracy. However, special loading programs, namely radial or proportional loading, allow great simplification in the equation governing plastic deformation, Eq. (13). For these cases, the normalized gradient to the yield surface, appearing on the right-hand side of that equation, becomes constant and no longer dependent on the history of past plastic deformation. For an important type of radial loading, the case of uniaxial stress, such as occurs during material testing, a closed form analytical solution may be obtained. This exact solution to rate-dependent plasticity gives an accessible picture of material behavior, allows various response parameters to be identified, and provides a measure of accuracy for the numerical solutions.

For a uniaxial stress state,

$$\sigma_{11} \neq 0, \ \dot{\sigma}_{11} \neq 0 \ , \quad \text{all others } \sigma_{ij} = \dot{\sigma}_{ij} = 0 \ ,$$

$$S_{11} = \frac{2}{3} \ \sigma_{11} \ , \tag{34}$$

$$S_{22} = S_{33} = - \ 1/2 \ S_{11} \ ,$$

$$\varepsilon^P_{22} = \varepsilon^P_{33} = - \ 1/2 \ \varepsilon^P_{11} \ ;$$

hence,

$$\varepsilon^P = \left| \varepsilon^P_{11} \right| \ ,$$

and

$$3/2 \ \frac{1}{\sigma_y} \ \frac{\partial f}{\partial \sigma_{11}} = \pm \ 1 \ ,$$

where the sign depends on the sign of the quantity ($S_{11} - \alpha_{11}$). (For uniaxial stress, the normal to the yield surface is a vector pointing in the positive or negative direction.)

Using the relations from Eq. (34) in Eq. (19), the equation governing the growth of plastic strain becomes

$$\frac{\sigma_o b}{\dot{\varepsilon}_o + \dot{\varepsilon}^P} \ \ddot{\varepsilon}^P + 3/2 \ C \ \dot{\varepsilon}^P = \dot{\sigma} \ , \tag{35}$$

where $\dot{\sigma} = \text{sign} \ (S_{11} - \alpha_{11}) \ \dot{\sigma}_{11}$.

Defining $\eta = \dot{\varepsilon}_o + \dot{\varepsilon}^P$,

so $\dot{\eta} = \ddot{\varepsilon}^P$,

Eq. (35) may be written

$$\sigma_o b \dot{\eta} + 3/2\ C \eta^2 - (\dot{\sigma} + 3/2\ C \dot{\varepsilon}_o)\ \eta = 0 \quad . \tag{36}$$

Eq. (36) is a Riccati equation with zero right-hand side, which, fortunately, may be solved in closed form by the substitution

$$\eta = \frac{1}{y} \quad , \quad \dot{\eta} = - \frac{\dot{y}}{y^2} \quad ,$$

giving

$$\sigma_o b \dot{y} + (\dot{\sigma} + 3/2\ C \dot{\varepsilon}_o)\ y = 3/2\ C \quad . \tag{37}$$

The complementary solution of Eq. (37) is obtained

$$\frac{dy}{y} = - \frac{1}{\sigma_o b} (\dot{\sigma} + 3/2\ C \dot{\varepsilon}_o)\ dt.$$

Integrating

$$\ell n\ y = C' - \frac{1}{\sigma_o b} (\sigma + 3/2\ C \dot{\varepsilon}_o t) \quad ,$$

or

$$y = C'' \exp \left[- \frac{1}{\sigma_o b} (\sigma + 3/2\ C \dot{\varepsilon}_o t) \right] \quad . \tag{38}$$

Allowing the constant of integration C'' to vary with time and substituting into Eq. (38) gives

$$\sigma_o b \exp \left[- \frac{1}{\sigma_o b} (\sigma + 3/2\ C \dot{\varepsilon}_o t) \right] \dot{C}'' = 3/2\ C \quad .$$

Integrating,

$$C'' = C_1 + \frac{3/2C}{\sigma_o b} \int \exp\left[\frac{1}{\sigma_o b}\left(\sigma + 3/2\ C\ \dot{\varepsilon}_o\ t\right)\right] dt.$$

Then, a complete solution to Eq. (35) may be written

$$\frac{1}{\dot{\varepsilon}^P + \dot{\varepsilon}_o} = \left\langle C_1 + \frac{3/2C}{\sigma_o b} \int \exp\left[\frac{1}{\sigma_o b}\left(\sigma + 3/2\ C\ \dot{\varepsilon}_o t\right)\right] dt \right\rangle \cdot \exp\left[-\frac{1}{\sigma_o b}\left(\sigma + 3/2\ C\ \dot{\varepsilon}_o t\right)\right] . \tag{39}$$

To proceed further, the variation of the stress σ with time must be specified. Since the application of interest will be stress loading rates appropriate to a stress-controlled uniaxial material testing machine, sufficient generality is obtained from piecewise linear loading histories in time. Thus,

$$\sigma = \Sigma_o + \dot{\Sigma}\, t \quad , \quad t \text{ in linear loading interval} ,$$

and (40)

$$\dot{\sigma} = \dot{\Sigma} = \text{constant} .$$

Using Eq. (40) in Eq. (39) gives a solution valid during any loading interval for which plastic strain is occurring

$$\frac{1}{\dot{\varepsilon}^P + \dot{\varepsilon}_o} = C_1 \exp\left[-\frac{\sigma + 3/2\ C\ \dot{\varepsilon}_o t}{\sigma_o b}\right] + \frac{1}{\dot{p} + \dot{\varepsilon}_o} , \tag{41}$$

where $\dot{p} = \dfrac{\dot{\Sigma}}{3/2C}$.

The parameter $\dot{p}$ in Eq. (41) is a steady state plastic strain rate corresponding to the constant stress rate in the loading interval; the plastic strain rate, $\dot{\varepsilon}^P$, asymptotically approaches this value. Integrating Eq. (41) gives the plastic strain

$$\varepsilon^P = C_2 + \dot{p}t + \frac{\sigma_o b}{3/2C} \ln\left(\frac{1}{\dot{\varepsilon}^P + \dot{\varepsilon}_o}\right) \tag{42}$$

in the loading interval.

The constants C_1 and C_2 appearing in Eqs. (41) and (42) are evaluated by requiring that the plastic strain rate and plastic strain be continuous between the previous loading interval and the present interval.

Some care is required in applying Eqs. (41) and (42) to a particular situation because of the sign conventions adopted during the derivation. Thus, the strain quantity calculated is equal to the absolute value of the plastic axial strain. Similarly, the stress rate quantity $\dot{\sigma}$ is positive or negative as the absolute magnitude of the stress is increasing or decreasing. This convention allows the quantities of Eqs. (41) and (42) to be calculated. The sign of the plastic strain developed will then depend on sign $(S_{11} - \alpha_{11})$. (For small strains this is merely the sign of the stress, tension or compression.)

Standard uniaxial material tests may also be performed on machines so that the strain or deformation rather than the stress or load is varied in a prescribed manner. Modern servohydraulic testing machines may control either quantity, so that stress or strain is prescribed at the experimentalist's discretion and the remaining quantity is determined as the result of the test.

In modeling a strain controlled test, the stress field is still uniaxial, so Eq. (35) applies;

$$\frac{\sigma_o b}{\dot{\varepsilon}_o + \dot{\varepsilon}^P} \ddot{\varepsilon}^P + 3/2\ C\ \dot{\varepsilon}^P = \dot{\sigma} \ . \tag{35}$$

However, the stress rate on the right-hand side is no longer known. This problem is avoided by writing, for uniaxial stress,

$$\dot{\sigma} = E\,\dot{\varepsilon}^e = E\left(\dot{\varepsilon} - \dot{\varepsilon}^P\right) \ . \tag{43}$$

Then Eq. (35) becomes

$$\frac{\sigma_o b}{\dot{\varepsilon}_o + \dot{\varepsilon}^P} \ddot{\varepsilon}^P + (3/2\ C + E)\,\dot{\varepsilon}^P = E\,\dot{\varepsilon} \ . \tag{44}$$

Eq. (44) may be solved in the same manner as the stress control process, once the strain rate loading has been specified. Again the prescribed strain

will be assumed to be piecewise linear; this is sufficient to model accurately most material testing conditions. So

$$\varepsilon = R_o + \dot{R}t \quad , \quad t \text{ in linear loading interval} \quad ,$$

and (45)

$$\dot{\varepsilon} = \dot{R} \quad \text{(a constant)} \quad .$$

The solution corresponding to the loading program of Eq. (45) is

$$\frac{1}{\dot{\varepsilon}_o + \dot{\varepsilon}^P} = \frac{1}{\dot{\varepsilon}_o + \dot{r}} + C_1' \exp\left[-\frac{E\,\varepsilon + (3/2\ C + \dot{E})\varepsilon_o t}{\sigma_o b}\right] \quad , \quad (46)$$

where

$$\dot{r} = \frac{E_T}{3/2\ C}\ \dot{R} \quad .$$

$\dot{r}$ corresponds to a steady state plastic strain rate for a constant strain rate loading $\dot{R}$. The actual plastic strain rate approaches this value asymptotically. $\dot{r}$ and $\dot{p}$ for the stress controlled test are entirely analogous terms.

Eq. (46) is integrated to give

$$\varepsilon^P = C_2' + \dot{r}\,t + \frac{\sigma_o b}{3/2\ C + E}\ \ell n\left(\frac{1}{\dot{\varepsilon}_o + \dot{\varepsilon}^P}\right) \quad . \quad (47)$$

Again, the constants C'_1 and C'_2 appearing in Eqs. (46) and (47) are evaluated by requiring that the plastic strain rate and plastic strain be continuous between intervals.

The two sets of equations, Eqs. (41) and (42) and Eqs. (46) and (47), give exact solutions for the plastic behavior of materials under actual, realistic testing conditions. As such, they allow easy determination of the shape of stress-strain curve for a wide variety of loading programs. In addition, the easily calculable solution serves as a check case for the more general structural analysis procedures.

IV. APPLICATIONS OF ONE-DIMENSIONAL MODEL

A. Constant Rate Tensile Testing

The uniaxial stress solutions to the equations of plastic deformation are used to model the constant strain rate material tests of the type illustrated by Figure 1. For the piecewise linear loading programs considered in Section III, the time origin is set to the beginning of the loading interval being considered. Hence the strain for this portion of the strain controlled test is given by Eq. (48),

$$\varepsilon = R_o + \dot{R}t \quad , \tag{48}$$

where $R_o = \varepsilon_I$ (initial strain in loading interval).

Both the plastic strain and plastic strain rate must be continuous. At the beginning of an interval, then, these variables must be equal to their value at the end of the previous interval.

$$\left.\begin{aligned} \dot{\varepsilon}^P &= \dot{\varepsilon}^P_I \\ \varepsilon^P &= \varepsilon^P_I \end{aligned}\right\} \qquad \text{at } t = 0 \quad . \tag{49}$$

For the initial interval, the time origin is set to the time when the stress reaches the static yield stress for the material and the plastic state is first entered. For this special interval

$$\varepsilon_I = \frac{\sigma_o}{E}$$

and (50)

$$\dot{\varepsilon}^P_I = \varepsilon^P_I = 0 \quad ,$$

since there can be no plastic strain before the yield surface is crossed.

Applying the initial conditions Eq. (49) to the solutions for constant strain rate uniaxial stress given by Eqs. (46 and 47) allows the constants to be determined as

$$C_1' = \frac{\dot{r} - \dot{\varepsilon}_I^P}{(\dot{\varepsilon}_o + \dot{\varepsilon}_I^P)(\dot{\varepsilon}_o + \dot{r})} \exp\left[\frac{E\,\varepsilon_I}{\sigma_o b}\right]$$

and (51)

$$C_2' = \varepsilon_I^P - \frac{\sigma_o b}{(3/2\ C + E)} \ln\left(\frac{1}{\dot{\varepsilon}_o + \dot{\varepsilon}_I^P}\right) .$$

Inserting these constants into the Eqs. (46) and (47) results in

$$\varepsilon^P = \varepsilon_I^P + \dot{r}t + \frac{\sigma_o b}{3/2\ C + E} \ln \left\langle \frac{\dot{\varepsilon}_o + \dot{\varepsilon}_I^P}{\dot{\varepsilon}_o + \dot{\varepsilon}^P} \right\rangle$$

and (52)

$$\frac{\dot{\varepsilon}_o + \dot{\varepsilon}_I^P}{\dot{\varepsilon}_o + \dot{\varepsilon}^P} = \frac{\dot{\varepsilon}_o + \dot{\varepsilon}_I^P}{\dot{\varepsilon}_o + \dot{r}} + \frac{\dot{r} - \dot{\varepsilon}_I^P}{\dot{\varepsilon}_o + \dot{r}} \exp\left[-\frac{E\dot{R} + (3/2\ C + E)\dot{\varepsilon}_o}{\sigma_o b}\, t\right] .$$

To obtain the stress-strain curve for this model of the uniaxial test, the values from Eq. (52) are inserted into

$$\sigma = E\,\varepsilon^e = E(\varepsilon - \varepsilon^P) \quad , \tag{53}$$

where $\varepsilon = \varepsilon_I + \dot{R}t$.

Finally, it is more convenient to eliminate the time and deal directly with the increase in strain since the start of the interval, as

$$t = \frac{\varepsilon - \varepsilon_I}{\dot{R}} = \frac{\Delta\varepsilon}{\dot{R}} \quad . \tag{54}$$

Then

$$\sigma = \sigma_I + E_T \Delta\varepsilon - \frac{\sigma_o b}{\frac{E}{E - E_T}} \ell n \left\langle \frac{\dot{\varepsilon}_o + \dot{\varepsilon}^P_I}{\dot{\varepsilon}_o + \dot{\varepsilon}^P} \right\rangle$$

and (55)

$$\frac{\dot{\varepsilon}_o + \dot{\varepsilon}^P_I}{\dot{\varepsilon}_o + \dot{\varepsilon}^P} = \frac{\dot{\varepsilon}_o + \dot{\varepsilon}^P_I}{\dot{\varepsilon}_o + \dot{r}} + \frac{\dot{r} - \dot{\varepsilon}^P_I}{\dot{\varepsilon}_o + \dot{r}} \exp \left[- \frac{E(\dot{\varepsilon}_o + \dot{r})}{\sigma_o b \dot{r}} \Delta\varepsilon \right] .$$

To demonstrate the use of Eq. (55), material parameters are obtained from Figure 1 and the experimental data from that series of tests modeled. The data are due to Lindholm[1] for Titanium 6 Al-4V alloy tested in tension at 70°F. The strain range will be restricted to 4% for the purpose of constructing the bilinear approximation for back extrapolation to determine yield stress. This process results in the data in Figure 3, where the yield stress-plastic strain rate curve to fit the experimental points is also shown. The relevant material properties obtained from Figures 1 and 3 are listed in Table 1.

TABLE 1. MATERIAL PROPERTIES FOR Ti 6Al-4V IN TENSION AT 70°F (REFERENCE (1))

Modulus

$E = 17{,}000{,}000$ psi $\qquad E_T = 350{,}000$ psi

Static Yield

$\sigma_o = 140{,}000$ psi $\qquad \varepsilon_o = .00824$

Rate Dependency

$\dot{\varepsilon}_o = .5/\text{sec} \qquad b = .0314$

Using these values in Eq. (55), along with the initial conditions for the first plastic interval Eq. (50), results in the model of the uniaxial constant strain rate test shown in Figure 4. Also shown in Figure 4 are the relevant data points from Figure 1. That the agreement between the model and experiment is excellent should not be surprising for this case, since the model was calibrated to this data. The errors are an indication of the accuracy of the bilinear approximation and the logarithmic yield stress-plastic strain rate fit.

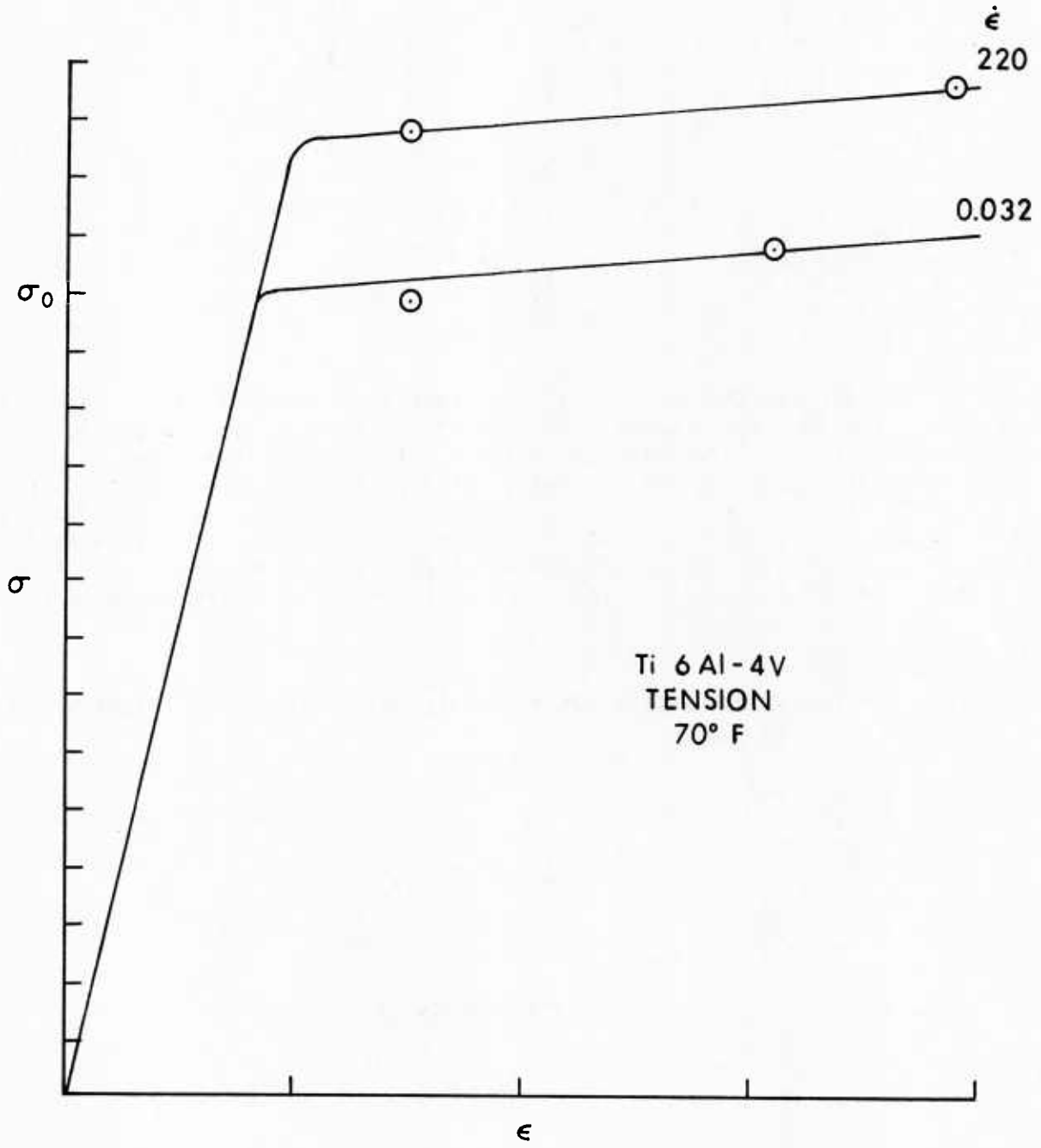

Figure 4. Model of Constant Strain Rate Uniaxial Tensile Test. Experimental Points from Reference (1)

The shape of the curves is very nearly that of the bilinear approximation; however, they do not have a sharp corner at the "dynamic" yield stress. Instead, they rise past the static yield stress at nearly the elastic slope. Then within a very narrow transition, e.g., in the high strain rate example, $\dot{\varepsilon}$ = 220/sec, the zone is less than .1% strain centered about 1% strain, the curve abruptly changes to the slope of the plastic region. This abruptness in the transition and rapid approach to a "steady state" plastic deformation rate is important to the validity of using constant strain rate tests to generate constant plastic strain rate data. The use of back extrapolation techniques to measure yield stresses assures that the values determined correspond to constant plastic strain rates.

After the model has been calibrated to the data of Figure 1, more complicated loading histories may be calculated. One such history which has been experimentally studied [9,18] is to load at a constant total strain rate into the plastic zone, and then to change abruptly to a different, but again constant, strain rate. This loading program may be easily modeled by Eq. (55), where now the (nonzero) values of plastic strain rate and plastic strains are used as initial conditions across the change of interval.

The results of these calculations are shown in Figure 5 for the same two constant strain rates as used in Figure 4. When the strain rate is suddenly increased from the lower to the higher rate, the stress-strain curve follows a nearly elastic slope initially. The curve again has a sharp transition and within a half of a percent strain has rejoined the stress-strain curve of a test performed entirely at the higher rate. When the strain rate is suddenly decreased from the higher to the lower rate, the curve falls along a nearly vertical line and transitions to the lower curve within a few hundredths of a percent strain. This behavior of the model reproduces the experimental data of References (9, 18) well.

Also shown in Figure 5 are the results of modeling a tensile test performed with stress control. The Eqs. (41) and (42) are used, along with the data of Table 1, to obtain this curve. During a stress control test, the stress rate of loading is controlled at a constant level by the machine. For comparison of data the stress rate should correspond to a particular constant strain rate. In the example of Figure 5 the stress rate is controlled to give the same steady state plastic strain rate as the upper curve of the strain control tests. As may be seen from the figure, the upper curves for stress and strain control do not correspond within the strain range considered. At larger strains the two curves coalesce. The stress control-test takes much longer to attain a steady plastic strain rate. This difference in the shape of the stress strain curve depending on the control of the testing machine has been noted in the References (9, 18).

B. Creep and Relaxation

It has been noted experimentally that creep and relaxation phenomena appear in metals at room temperature when they are stressed above their yield stress.[9,10] These phenomena are due to the plastic deformation requiring time to develop fully. The suppression of a part of the plastic deformation is what raises the stress-strain curve at real loading rates above the static curve. A corollary is that, if the load rate is stopped and the stress held

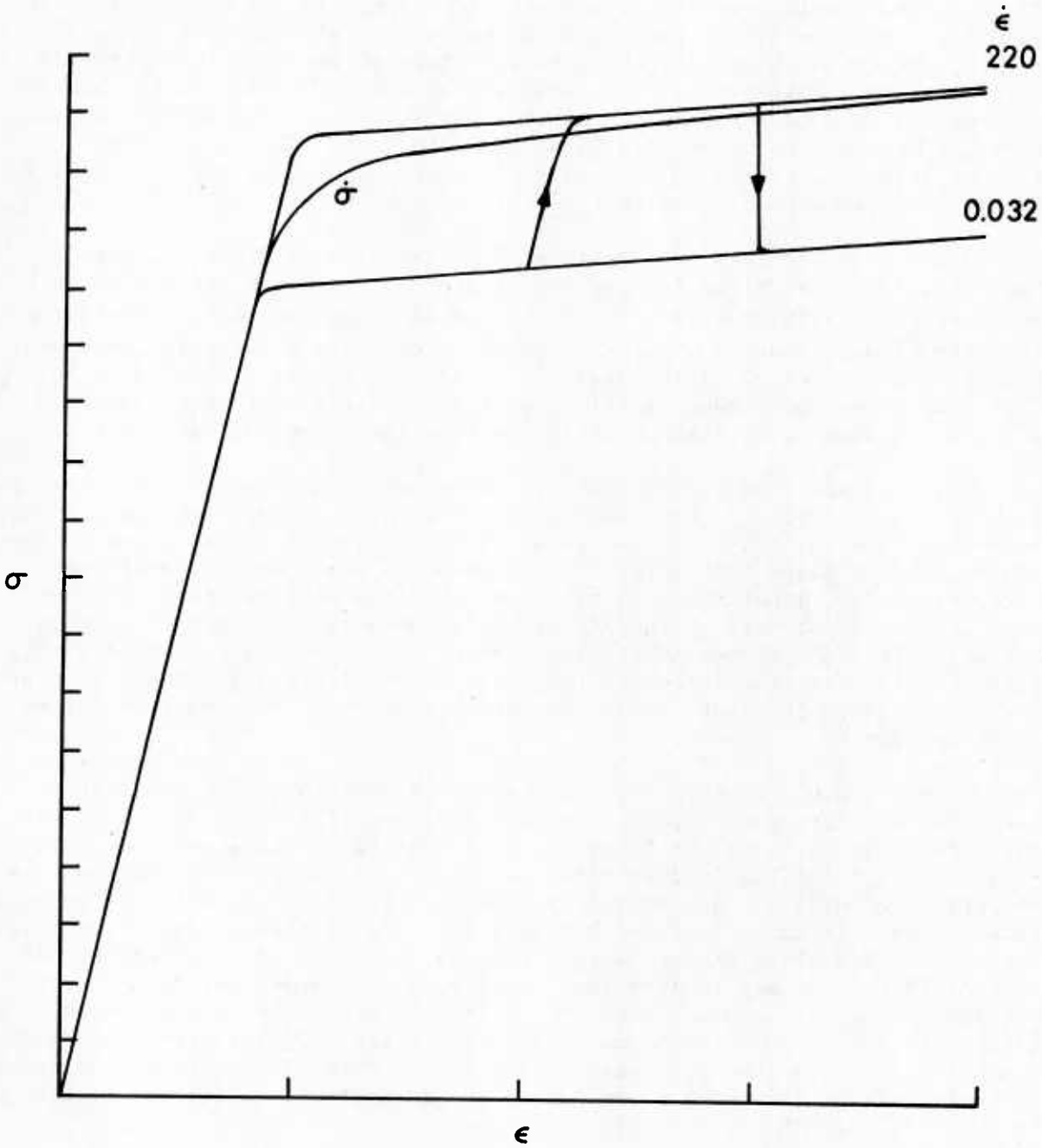

Figure 5. Application of Model of Uniaxial Stress Plastic Deformation to Change of Strain Rate and to Stress Rate Control

constant, the remainder of the suppressed plastic deformations will eventually occur. This process is creep.

The creep phenomenon is modeled with Eqs. (41) and (42). The material is presumed to be loaded into the plastic range by some program, and the response is calculated by the methods of Section A. Then the loading is halted and the stress maintained constant at the current value. The period of constant stress is taken as an interval, with conditions

$$\begin{aligned} \dot{\varepsilon}^P &= \dot{\varepsilon}^P_I \\ \varepsilon^P &= \varepsilon^P_I \qquad \text{at } t = 0 , \\ \sigma &= \sigma_I \end{aligned} \tag{56}$$

and

$$\dot{\Sigma} = \dot{p} = 0 .$$

Then the response of the material is given by

$$\varepsilon = \varepsilon_I + \frac{\sigma_o b}{3/2\ C}\ \ell n\ \left\langle \frac{\dot{\varepsilon}_o + \dot{\varepsilon}^P_I}{\dot{\varepsilon}_o + \dot{\varepsilon}^P} \right\rangle \tag{57}$$

with

$$\frac{\dot{\varepsilon}_o + \dot{\varepsilon}^P_I}{\dot{\varepsilon}_o + \dot{\varepsilon}^P} = 1 + \frac{\dot{\varepsilon}^P_I}{\dot{\varepsilon}_o} - \frac{\dot{\varepsilon}^P_I}{\dot{\varepsilon}_o} \exp\left[- \frac{3/2\ C\ \dot{\varepsilon}_o}{\sigma_o b}\ t \right] ,$$

and

$$\sigma = \sigma_I .$$

Thus, under a constant stress, the strain grows as indicated by Eq. (57). The

maximum strain is approached as time goes to infinity; then the exponential term approaches zero and

$$\frac{\sigma_o b}{3/2\ C}\ \ell n\ \left\langle 1 + \frac{\dot{\varepsilon}^P_I}{\dot{\varepsilon}_o} \right\rangle = \frac{\sigma_y - \sigma_o}{3/2\ C}\ , \tag{58}$$

where σ_y is the initial yield stress corresponding to a constant plastic strain rate of $\dot{\varepsilon}^P_I$. Since the tangent modulus at any plastic strain rate is parallel to the static value, the stress difference does not change in proceeding to higher initial strain values. From Figure 2 and Eq. (58) then, the material will creep at constant stress until it reaches the static stress-strain curve. The approach to this curve is very rapid, being governed by the exponential term of Eq. (57). For the material properties of Ti 6Al-4V alloy being utilized in the previous calculations, all but 2% of the total creep would have occurred within .1 sec.

By the same considerations as were applied to modeling the creep behavior of a material above the yield stress, the relaxation phenomena may be calculated. In this case the strain is held constant after an initial loading into the plastic zone, and the stress decreases with time until the static stress-strain curve is reached.

V. ASPECTS OF RATE-DEPENDENT PLASTICITY

A. Behavior of the Model in Multiaxial Stress Space

The concepts of stress space, yield surface, and loading trajectory were introduced in Section II.B. The current section will describe the behavior of the rate-dependent model during plastic deformation.

Interior to the initial yield surface is a volume of stress space which corresponds to purely elastic material behavior. As the load increases, the stress point approaches the yield surface and eventually touches it. It is convenient to think of the material as having entered the plastic state at this time. Since the initial yield surface is static (i.e., it corresponds to $\dot{\varepsilon}^P = 0$), there is no plastic strain occurring at this instant. Thus continuity of behavior is preserved between elastic and plastic states.

As the load continues to increase, a finite plastic strain rate will develop, giving rise to plastic strains. The stress point is now located on a yield surface corresponding to $\dot{\varepsilon}^P > 0$. Concentric to and interior to this surface is a current static yield surface. As plastic strain develops, these concentric surfaces are shifted by the kinematic hardening rules. This behavior is shown in Figure 6.

The outer current yield surface expands and contracts about the inner static surface depending on the instantaneous value of the plastic strain rate. As long as the stress point is outside of the static surface, plastic deformation is occurring and tests to determine loading, unloading, or neutral loading conditions, as in the classical theory, are unnecessary. If the

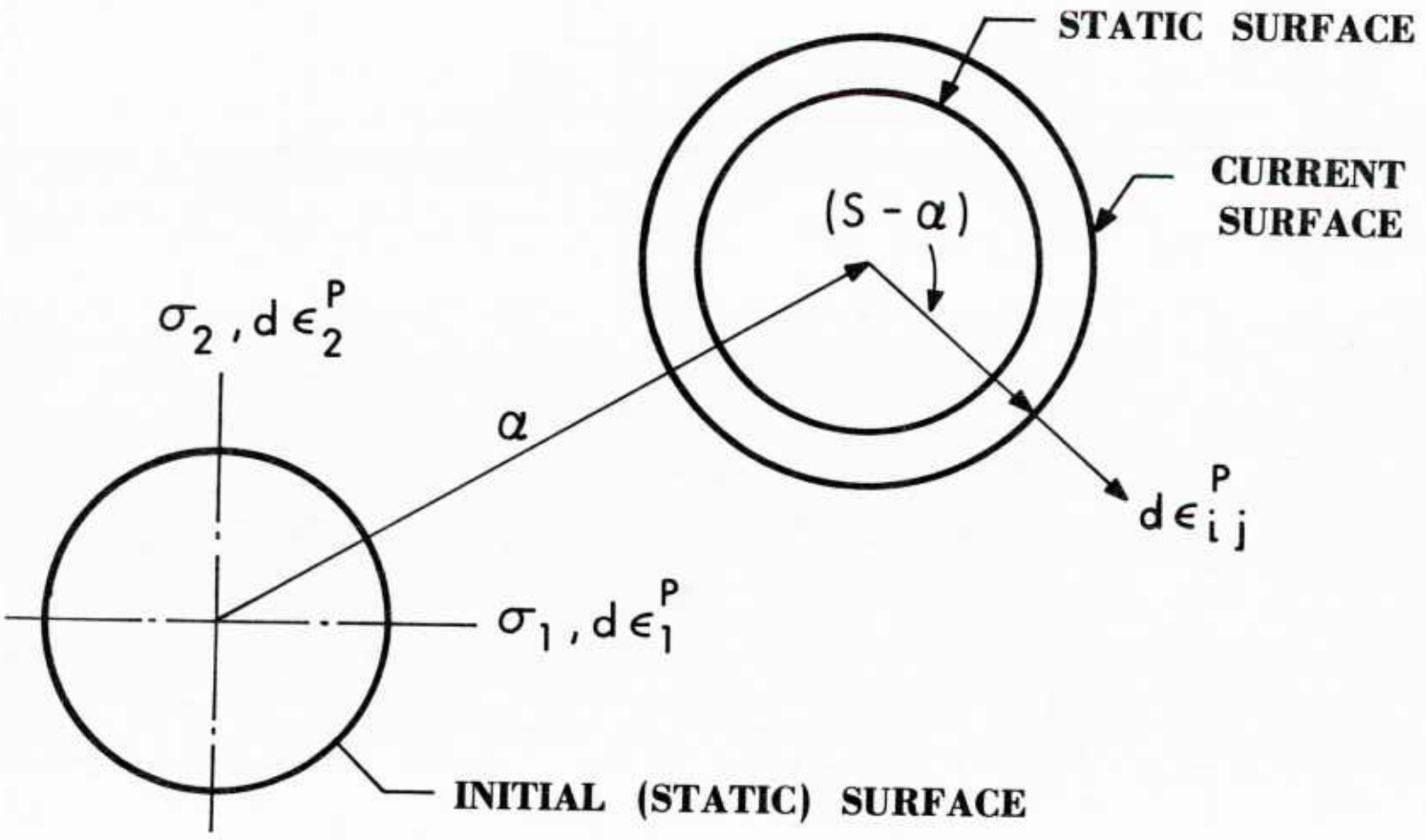

Figure 6. Behavior of Yield Surface During Plastic Deformation

loading program is such that the current yield surface shrinks to the static surface, plastic deformation will cease since $\dot{\varepsilon}^P = 0$, but the plastic state will not be exited until the stress point moves interior to the static surface.

What is referred to as neutral loading in the classical theory is the movement of the stress point on the static surface. No plastic deformation can result from this type of process, due to the vanishing of $\dot{\varepsilon}^P$ on this surface.

B. Existence of Equation of State

The behavior of materials to uniaxial tests where the strain rate is changed abruptly, as in Section IV.A, is often regarded as proof of the nonexistence of an equation of state for plastic deformation.[24] This behavior is shown in Figure 7, which reproduces the stress-strain curves of a material at two different constant strain rates $\dot{\varepsilon}_1$ and $\dot{\varepsilon}_2$, as well as the case where the strain rate is changed from $\dot{\varepsilon}_1$ to $\dot{\varepsilon}_2$. Here, for the same value of strain corresponding to the vertical line and the same value of strain rate, $\dot{\varepsilon}_2$, there are two values of stress possible, shown by the points (a) and (b). This nonuniqueness of the stress is taken as evidence for the nonexistence of an equation of state appropriate to plastic flow. It is argued that the past history of the material must be known, i.e., the stress-strain curve up to the present time, in order to make the stress unique for a given strain and strain rate.

An alternate approach is to consider a different set of variables to define the state of the material. In particular, the variable used in the present theory, the plastic strain rate, eliminates the preceding difficulty. Lines of constant plastic strain rate are parallel to the tangent modulus of the material; their intersection with lines of constant strain give unique points which determine the stress. After an abrupt change of strain rate, the plastic strain rate increases steadily in the manner prescribed by Eq. (46), toward an upper limit. Thus the instantaneous value of this quantity stores the relevant rate history information required to determine the stress uniquely. This consideration is an additional argument for use of plastic strain rate in the formulation of the rate-dependent theory.

The above consideration is not meant to imply that the present theory is history independent. Although the instantaneous value of the plastic strain rate is all that is required, the determination of this quantity required the solving of a differential equation with initial conditions. Thus all past history is included in the current value of this internal state variable.

---

[24] *A.M. Freudenthal, The Inelastic Behavior of Engineering Materials and Structures, John Wiley and Sons, NY, 1950.*

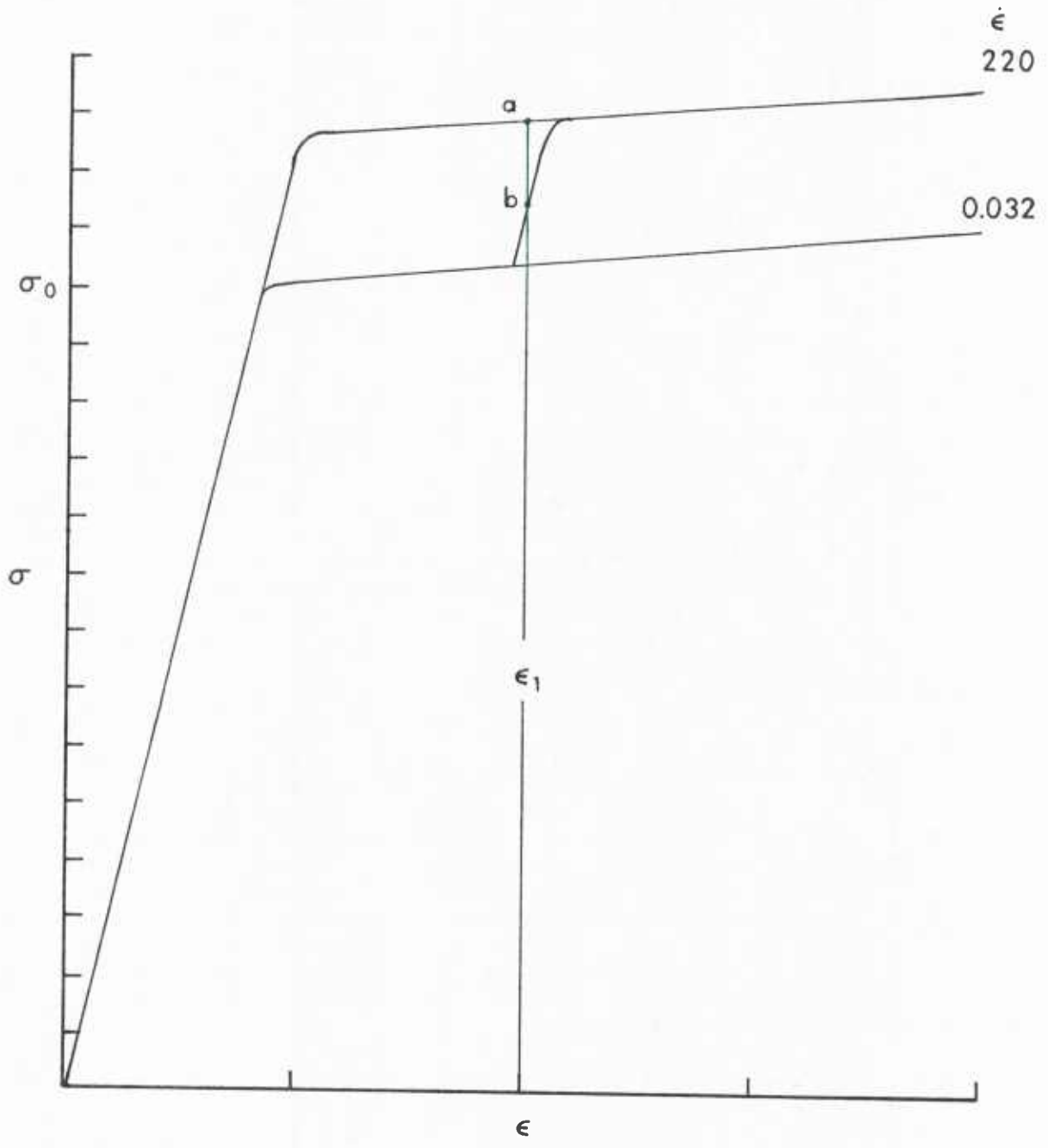

Figure 7. Existence of Equation of State for Plastic Flow

C. Relation to Viscoplasticity

A question arises as to the relation of the present rate-dependent plasticity theory and the theory of viscoplasticity as expounded, e.g., by Perzyna.[21] There appears to be no simple answer. The approaches to the derivation of the theory were different, and the resulting equations for the general case cannot be put into similar forms. The relationship between the theories is a matter deserving additional study.

In one special case, however, the resulting equations reduce to the same form. This is the case of a perfectly plastic material, where the plastic modulus is zero and no strain hardening occurs. Eq. (33), written for uniaxial stress conditions, becomes

$$\dot{\varepsilon}^P = \dot{\varepsilon}_o \left\langle \exp\left[\frac{\sigma - \sigma_o}{\sigma_o b}\right] - 1 \right\rangle \quad . \tag{59}$$

By comparison to Eq. (2.90) of Reference (21), this special case of rate-dependent plasticity is seen to be identical with the exponential form of classical viscoplasticity. Viscoplasticity is derived from the concept of a function of the overstress, here represented by the quantity $\sigma - \sigma_o$, and a viscosity coefficient characteristic of the material. Comparison of the equations reveals that the quantity $\dot{\varepsilon}_o$, representing a transition strain rate, as in Figure 3 in the present theory, appears in the same place as the viscosity coefficient, γ, of classical viscoplasticity.

D. Conclusion

A form of the equations of plasticity has been derived which allows for rate-dependent phenomena. The major assumption was simply that the yield surface depended on the plastic strain rate. The choice of plastic strain rate as the rate variable was based on physical considerations and on appropriateness as an internal state variable. From this assumption the governing equations were determined by extension of classical plasticity methods without recourse to additional assumptions concerning overstress or material viscosity. The theory as derived contains rate-independent plasticity as a limiting case when rate effect vanishes; therefore, it may serve as a matrix to relate the various elements of rate dependency, creep and relaxation, and classical plasticity.

A factor ignored in the present theory but clearly of importance is temperature. Elementary forms of temperature dependence on yield stress may be added to the present formulation in the same manner that these effects were added to the rate-independent plasticity in Reference (19).

When high strain rates are combined with large strains, the heat generated by the plastic work raises the temperature sufficiently to affect the plastic deformation mechanism.[13] This thermo-mechanical coupling would be an important component of any theory attempting to explain impact or penetration phenomena, for example. It is obvious that the addition of this type of coupling to a rate-dependent theory of plasticity would be a major

modification, if handled in a rigorous manner. A temperature modified rate-dependent formulation would be the optimum starting point to derive such theory.

On a more modest scale of effort, the connection between this theory and the theories of viscoplasticity should be investigated for the general case. Identification of areas of similarity or difference could help in the classification of the theories, and might lead to further interesting congruences, as was observed between the material viscosity of viscoplasticity and the transition strain rate of the present development.

Comparison of the results of calculations with multiaxial states of stress to experimental data may reveal other areas where rate effects appear. For example, attempting to load a specimen along a Von Mises ellipse in a torsion/tension test leads to a bulge in the curve, which is matched by a rate-dependent calculation.[25] Additional study of the apparent shape of the yield surface under variation of plastic strain rate, as well as stress state, may lead to new understanding of experimental yield surface data.

---

[25] *S.A. Meguid, L.E. Malvern, J.D. Campbell, "Plastic Flow of Mild Steel Under Proportional and Non-proportional Straining at a Controlled Rate," Journal of Engineering Materials and Technololgy, Proceedings of ASME Vol. 101, pp 248-253, July 1979.*

REFERENCES

1. U.S. Lindholm, L.M. Yeakley, R.L. Bessey, "An Investigation of the Behavior of Materials Under High Rates of Deformation," Air Force Materials Laboratory TR-68-194, Wright-Patterson AFB, OH, July 1968.

2. U.S. Lindholm, R.L. Bessey, "A Survey of Rate Dependent Strength Properties of Metals," Air Force Materials Laboratory TR-69-119, Wright-Patterson AFB, OH, April 1969.

3. A.J. Holzer, "A Tabular Summary of Some Experiments in Dynamic Plasticity," Journal of Engineering Materials and Technology, Vol. 101, pp 231-237, July 1979.

4. U.F. Kocks, "Constitutive Relations for Slip," Constitutive Equations in Plasticity, ed. A.S. Argon, MIT Press, Cambridge, MA, 1975.

5. J.M. Kelly and P.G. Gillis, "The Influence of a Limiting Dislocation Flux on the Mechanical Response of Polycrystalline Metals," International Journal of Solids and Structures, Vol. 10, pp 45-59, 1974.

6. A.S. Argon, "Physical Basis in Constitutive Equations for Inelastic Deformation," Constitutive Equations in Plasticity, ed. A.S. Argon, MIT Press, Cambridge, MA, 1975.

7. E.H. Lee, "Some Comments on Elastic-Plastic Analysis," International Journal of Solids and Structures, Vol. 17, pp 859-872, 1981.

8. M.F. Ashby and H.J. Frost, "The Kinetics of Inelastic Deformation Above 0°K," Constitutive Equations in Plasticity, ed. A.S. Argon, MIT Press, Cambridge, MA, 1975.

9. E. Krempl, "An Experimental Study of Room-Temperature Rate-Sensitivity, Creep and Relaxation of AISI Type 304 Stainless Steel," Journal of Mechanics and Physics of Solids, Vol. 27, pp 363-375, 1979.

10. A. Phillips, "The Foundations of Plasticity," Plasticity in Structural Engineering-Fundamentals and Applications, Springer-Verlag, NY, 1979.

11. S.R. Bodner and Y. Partom, "Constitutive Equations for Elastic - Viscoplastic Strain-Hardening Materials," Journal of Applied Mechanics, Vol. 42, pp 385-389, June 1975.

12. F.A. McClintock and A.S. Argon, eds., Mechanical Behavior of Materials, Addison-Wesley Publishing Co., Reading, MA, 1966.

13. O.W. Dillon, Jr., "Some Experiments in Thermoviscoplasticity," Constitutive Equations in Viscoplasticity: Phenomenological and Physical Aspects, AMD-Vol. 21, American Society of Mechanical Engineers, NY, 1976.

14. J.B. Martin, Plasticity: Fundamentals and General Results, MIT Press, Cambridge, MA, 1975.

REFERENCES (continued)

15. A. Mendelson, Plasticity: Theory and Application, Macmillan Co., NY, 1968.

16. J.R. Rice, "On the Structure of Stress-Strain Relations for Time-Dependent Plastic Deformation in Metals," Journal of Applied Mechanics, Vol. 37, pp 728-737, September 1970.

17. W. Olszak, "Generalized Yield Criteria for Advanced Models of Material Response," Plasticity in Structural Engineering Fundamentals and Applications, Springer-Verlag, NY, 1979.

18. D. Kujawski and E. Krempl, "The Rate (Time) - Dependent Behavior of Ti - 7Al-2 Cb - 1 Ta Titanium Alloy at Room Temperature Under Quasistatic Monotonic and Cyclic Loading," Journal of Applied Mechanics, Vol. 48, pp 55-63, March 1981.

19. C.E. Pugh, J.M. Corum, K.C. Lin and W.L. Greenstreet, "Currently Recommended Constitutive Equations for Inelastic Design Analysis of FFTF Components," ORNL-TM-3602, Oak Ridge National Lab., TN, September 1972.

20. K.J. Bathe, "Static and Dynamic Geometric and Material Nonlinear Analysis Using ADINA," Report 82448-2, Mass. Inst. of Tech., Cambridge, MA, May 1977.

21. P. Perzyna, "Fundamental Problems in Viscoplasticity," Advances in Applied Mechanics, ed. by G. Kuerti, Academic Press, NY, 1966.

22. P. Perzyna, "Thermodynamics of Dissipative Materials," Recent Developments in Thermomechanics of Solids, Springer-Verlag, NY, 1980.

23. A.R. Zak, "Finite Element Model for Nonaxisymmetric Structure with Rate Dependent Yield Conditions," BRL Contractor Report, In preparation.

24. A.M. Freudenthal, The Inelastic Behavior of Engineering Materials and Structures, John Wiley and Sons, NY, 1950.

25. S.A. Meguid, L.E. Malvern, J.D. Campbell, "Plastic Flow of Mild Steel Under Proportional and Non-proportional Straining at a Controlled Rate," Journal of Engineering Materials and Technology, Proceedings of ASME Vol. 101, pp 248-253, July 1979.

DISTRIBUTION LIST

No. of Copies	Organization
12	Administrator Defense Technical Info Center ATTN: DTIC-DDA Cameron Station Alexandria, VA 22314
1	Director of Defense Research & Engineering (OSD) ATTN: R. Thorkildsen Washington, DC 20301
1	Director of Defense Research & Engineering (OSD) ATN: J. Persh Washington, DC 20301
1	Director Defense Advanced Research Projects Agency 1400 Wilson Boulevard Arlington, VA 22209
1	Director Institute of Defense Analyses ATTN: Documents Acquisition 1801 Beauregard Street Alexandria, VA 22311
1	HQDA (DAMA-MS) Washington, DC 20310
1	HQDA (DAMA-ZA) Washington, DC 20310
1	HQDA (DAMA-ZD), H. Woodall Washington, DC 20310
1	HQDA (DAMA-ART-M) Washington, DC 20310
2	HQDA (DAMA-CSM-VA) (DAMA-CSM-CA) Washington, DC 20310
1	Commander US Army Materiel Development and Readiness Command ATTN: DRCDMD-ST 5001 Eisenhower Avenue Alexandria, VA 22333
1	Commander US Army Materiel Development and Readiness Command ATTN: DRCLDC 5001 Eisenhower Avenue Alexandria, VA 22333
1	Commander US Army Materiel Development and Readiness Command ATTN: DRCDE Deputy Director 5001 Eisenhower Avenue Alexandria, VA 22333
1	Commander US Army Materiel Development and Readiness Command ATTN: DRCDE-R 5001 Eisenhower Avenue Alexandria, VA 22333
1	Commander US Army Materiel Development and Readiness Command 5001 Eisenhower Avenue Alexandria, VA 22333
8	Commander ARDC, USA AMCCOM ATTN: DRSMC-LCA(D), A. Moss DRSMC-LC(D) DRSMC-SE(D) DRSMC-SA(D) DRSMC-AC(D) DRSMC-LCU-SE(D) J. Pearson DRSMC-LCA-M(D), F. Saxe DRSMC-LCU-SS(D) R. Botticelli Dover, NJ 07801

DISTRIBUTION LIST

No. of Copies	Organization
5	Commander ARDC, USA AMCCOM ATTN: DRSMC-SCS(D) (2 cys) DRSMC-SCS-E(D) DRSMC-SCF(D) (2 cys) Dover, NJ 07801
1	Commander US Army Missile Command ATTN: DRSMI-YDL Redstone Arsenal, AL 35898
2	Commander ARDC, USA AMCCOM ATTN: DRSMC-TSS(D) Dover, NJ 07801
5	Commander ARDC, USA AMCCOM ATTN: DRSMC-TD(D) DRSMC-TDA(D) DRSMC-TDS(D) DRSMC-TDC(D) DRSMC-TDC(D), C. Larson Dover, NJ 07801
7	Commander ARDC, USA AMCCOM ATTN: DRSMC-LCA(D), B. Knutelski DRSMC-LCR-R(D), E.H. Moore III DRSMC-LCS(D), J. Gregorits DRSMC-LCS-D(D), K. Rubin DRSMC-LCA(D), T. Davidson DRSMC-LCA(D), E. Friedman DRSMC-LCA(D), A. Lehberger Dover, NJ 07801
1	Director US Army Air Mobility Research and Development Laboratory Ames Research Center Moffett Field, CA 94035
5	Commander ARDC, USA AMCCOM ATTN: DRSMC-LCU(D) E. Barrieres DRSMC-LCU(D) R. Davitt DRSMC-LCU-M(D) D. Robertson DRSMC-LCU-M(D) M. Weinstock DRSMC-LCA-M(D) C. Larson Dover, NJ 07801
7	Commander ARDC, USA AMCCOM ATTN: DRSMC-SCA(D) C.J. McGee DRSMC-SCA(D) S. Goldstein DRSMC-SCA(D), F.P. Puzychki DRSMC-SCA(D), E. Jeeter DRSMC-SCF(D) M.J. Schmitz DRSMC-SCF(D), L. Berman DRSMC-SCZ(D) P. Petrella Dover, NJ 07801
9	Commander ARDC, USA AMCCOM ATTN: DRSMC-SCM(D) DRSMC-SCM(D), E. Bloore DRSMC-SCM(D) J. Mulherin DRSMC-SCS(D) B. Brodman DRSMC-SCS(D), T. Hung DRSMC-SCA(D) W. Gadomski DRSMC-SCA(D) E. Malatesta DRSMC-SCA-T(D) P. Benzkofer DRSMC-SCA-T(D) F. Dahdouh Dover, NJ 07801

DISTRIBUTION LIST

No. of Copies	Organization
3	Commander ARDC, USA AMCCOM ATTN: DRSMC-LCA(D) W. Williver DRSMC-LCA(D) S. Bernstein DRSMC-LCA(D) G. Demitrack Dover, NJ 07801
4	Commander ARDC, USA AMCCOM ATTN: DRSMC-LCA(D), S. Yim DRSMC-LCA(D) L. Rosendorf DRSMC-LCA(D), S.H. Chu DRSMC-LCW(D), R. Wrenn Dover, NJ 07801
6	Director Benet Weapons Laboratory Armament R&D Center USA AMCCOM ATTN: DRSMC-LCB-TL(D) DRSMC-LCB(D) DRSMC-LCB-RA(D) R. Scanlon DRSMC-LCB-RM(D) M. Scarullo DRSMC-LCB-RA(D) R. Soanes, Jr. DRSMC-LCB-RA(D) J. Vasilakis Watervliet, NY 12189
7	Director USA AMCCOM Benet Weapons Laboratory ATTN: DRSMC-LCB-RA(D) T. Simkins DRSMC-LCB-D(D) J. Zweig DRSMC-LCB-RA(D) G. Pflegl DRSMC-LCB-M(D) J. Purtell DRSMC-LCB-RA(D) R. Racicot DRSMC-LCB-DS(D) J. Santini DRSMC-LCB-RA(D), J. Wu Watervliet, NY 12189

No. of Copies	Organization
2	Commander ARDC, USA AMCCOM ATTN: DRSMC-SC(D) DRSMC-SC(D) B. Shulman Dover, NJ 07801
2	Commander ARDC, USA AMCCOM ATTN: Army Fuze Mgt Project Office DRSMC-FU(D) Dover, NJ 07801
2	Commander ARDC, USA AMCCOM ATTN: DRSMC-DP(D) Development Project Office for Selected Ammunitions Dover, NJ 07801
2	Commander ARDC, USA AMCCOM ATTN: Product Assurance Directorate DRSMC-QA(D) Dover, NJ 07801
1	Commander ARDC, USA AMCCOM ATTN: DRSMC-NS(D) Dover, NJ 07801
1	Commander ARDC, USA AMCCOM ATTN: L. Goldsmith Dover, NJ 07801
1	Commander USA Armament, Munitions & Chem Cmd ATTN: DRSMC-TSE-SW(R) R. Radkiewicz Rock Island, IL 61299
2	Commander USA Armament, Munitions & Chem Cmd ATTN: DRSMC-LEP-L(R) DRSMC-TSE-SW(R), G. Strahl Rock Island, IL 61299

DISTRIBUTION LIST

No. of Copies	Organization
1	Commander USA Armament, Munitions & Chem Cmd ATTN: SARRI-RLS(R) Rock Island, IL 61299
1	Commander USA Aviation Research and Development Command ATTN: DRDAV-E 4300 Goodfellow Blvd St. Louis, MO 63120
2	Director USA Air Mobility Research and Development Laboratory ATTN: Hans Mark R.L. Cohen Ames Research Center Moffett Field, CA 94035
2	Director USA Research and Technology Laboratories Ames Research Center Moffett Field, CA 94035
2	Director USA Research and Technology Laboratories ATTN: DAVDL-AS DAVDL-AS Ames Research Center Moffett Field, CA 94035
1	Commander USA Communications Research and Development Command ATTN: DRSEL-ATDD Fort Monmouth, NJ 07703
1	Commander USA Electronics Research and Development Command Technical Support Activity ATTN: DELSD-L Fort Monmouth, NJ 07703
1	Commander Atmospheric Sciences Lab ATTN: DELAS-EO-MO, R. B. Gomez White Sands Missile Range NM 88002
3	Commander USA Harry Diamond Lab ATTN: DELHD-I-TR, H.D. Curchak DELHD-I-TR, H. Davis DELHD-S-QE-ES, Ben Banner 2800 Powder Mill Road Adelphi, MD 20783
1	Commander USA Harry Diamond Labs ATTN: DELHD-TA-L 2800 Powder Mill Road Adelphi, MD 20783
1	Director Night Vision Laboratory Fort Belvoir, VA 22060
1	Commander USA Missile Command ATTN: DRSMI-R Redstone Arsenal, AL 35898
2	Commandant USA Infantry School ATTN: ATSH-CD-CSO-OR Fort Benning, GA 31905
1	Commander USA Missile Command ATTN: DRCPM-TO Redstone Arsenal, AL 35898
1	Commander USA Mobility Equipment Research & Development Cmd Fort Belvoir, VA 22060

DISTRIBUTION LIST

No. of Copies	Organization
3	Commander USA Tank Automotive Cmd ATTN: DRSTA-TSL DRSTA-ZSA, R. Beck DRSTA-NS Warren, MI 48090
1	Commander USA Natick Research and Development Lab ATTN: DRDNA-DT Natick, MA 01760
1	Director USA TRADOC Systems Analysis Activity ATTN: ATAA-SL White Sands Missile Range NM 88002
2	President USA Armor and Engineer Board ATTN: ATZK-AE-CV ATZK-AE-IN, L. Smith Fort Knox, KY 40121
3	Commander USA Research Office ATTN: R. Weigle E. Saibel J. Chandra P.O. Box 12211 Research Triangle Park NC 27709
3	Commander USA Research Office ATTN: Technical Director, Engineering Div, Metallurgy & Materials Div P. O. Box 12211 Research Triangle Park NC 27709
4	Director USA Materials and Mechanics Research Center ATTN: Director (3 cys) DRXMR-ATL (1 cy) Watertown, MA 02172
2	Commander USA Materials and Mechanics Research Center ATTN: J. Mescall Technical Library Watertown, MA 02172
1	Commander USA Training and Doctrine Command ATTN: TRADOC Lib Fort Monroe, VA 23651
1	Commandant USA Armor School ATTN: Armor Agency, MG Brown Fort Knox, KY 40121
1	Commandant USA Field Artillery School ATTN: Field Artillery Agency Fort Sill, OK 73503
1	Superintendent Naval Postgraduate School ATTN: Dir of Lib Monterey, CA 93940
1	Commander USA Combined Arms Combat Development Activity Fort Leavenworth, KS 66027
1	Commander USA Combat Development Experimentation Command ATTN: Tech Info Center Bldg. 2925, Box 22 Fort Ord, CA 93941

DISTRIBUTION LIST

No. of Copies	Organization
1	Commander Naval Sea Systems Command Washington, DC 20360
1	Commander Naval Sea Systems Command (SEA-62R41) ATTN: L. Pasiuk Washington, DC 20360
1	Commander Naval Research Laboratory ATTN: Commander H. Peritt, Code R31 Washington, DC 20375
1	Commander David W. Taylor Naval Ship Research and Development Center Bethesda, MD 20084
4	Commander Naval Research Laboratory ATTN: W.J. Ferguson C. Sanday H. Pusey Tech Library Washington, DC 20375
6	Commander Naval Surface Weapons Center ATTN: Code X211, Lib E. Zimet, R13 R.R. Bernecker, R13 J.W. Forbes, R13 S.J. Jacobs, R10 K. Kim, R13 Silver Spring, MD 20910
3	Commander Naval Surface Weapons Center ATTN: Code E-31, R.C. Reed M.T. Walchak Code V-14, W.M. Hinckley Silver Spring, MD 20910
5	Commander Naval Surface Weapons Center ATTN: Code G-33, T.N. Tschirn Code N-43, J.J. Yagla L. Anderson G. Soo Hoo Code TX, W.G. Soper Dahlgren, VA 22448
1	Commander Naval Weapons Center China Lake, CA 93555
1	Commander Naval Weapons Center ATTN: J. O'Malley China Lake, CA 93555
2	Commander Naval Weapons Center ATTN: Code 3835, R. Sewell Code 3431, Tech Lib China Lake, CA 93555
2	Commander US Naval Weapons Center ATTN: Code 608, R. Derr Code 4505, C. Thelen China Lake, CA 93555
3	Commander Naval Weapons Center ATTN: Code 4057 Code 3835, B. Lundstrom Code 3835, M. Backman China Lake, CA 93555
1	Commander Naval Ordnance Station Indian Head, MD 20640
2	Commander Naval Ordnance Station ATTN: Code 5034, Ch. Irish T.C. Smith Indian Head, MD 20640

DISTRIBUTION LIST

No. of Copies	Organization
1	Office of Naval Research ATTN: Code ONR 439, N. Perrone Department of the Navy 800 North Quincy Street Arlington, VA 22217
1	Commandant US Marine Corps ATTN: AX Washington, DC 20380
1	AFATL/DLXP ATTN: W. Dittrich Eglin AFB, FL 32542
1	AFATL/DLD ATTN: D. Davis Eglin AFB, FL 32542
2	ADTC/DLJW Eglin AFB, FL 32542
1	ADTC/DLODL, Tech Lib Eglin AFB, FL 32542
1	AFWL/SUL Kirtland AFB, NM 87117
1	AFWL/SUL ATTN: J.L. Bratton Kirtland AFB, NM 87117
1	AFML/LLN (T. Nicholas) Wright-Patterson AFB OH 45433
1	ASD (XROT, G. Bennet) Wright-Patterson AFB OH 45433
2	Battelle Memorial Institute ATTN: L.E. Hulbert J.E. Backofen, Jr. 505 King Avenue Columbus, OH 43201
3	Battelle Pacific Northwest Laboratory ATTN: E.M. Patton F.A. Simonen L.A. Strope P.O. Box 999 Richland, WA 99352
1	Bell Telephone Labs. Inc. Mountain Avenue Murray Hill, NJ 07971
1	Director Lawrence Livermore Laboratory P.O. Box 808 Livermore, CA 94550
2	Director Lawrence Livermore Laboratory ATTN: E. Farley, L9; D. Burton, L200 P.O. Box 808 Livermore, CA 94550
3	Director Lawrence Livermore Laboratory ATTN: R.H. Toland, L-424 M.L. Wilkins; R. Werne P.O. Box 808 Livermore, CA 94550
1	Director NASA - Ames Research Center Moffett Field, CA 94035
2	Director Forrestal Research Center Aeronautical Engineering Lab ATTN: S. Lam; A. Eringen Princeton, NJ 08540
1	Director Sandia National Laboratory Livermore Laboratory ATTN: D. E. Waye P.O. Box 969 Livermore, CA 94550

DISTRIBUTION LIST

No. of Copies	Organization
1	Aircraft Armaments Inc. ATTN: John Hebert P.O. Box 126 Cockeysville, MD 21030
2	ARES, Inc. ATTN: Duane Summers Phil Conners Port Clinton, OH 43452
2	AVCO Coroporation Structures and Mechanics Dept ATTN: W. Broding; J. Gilmore 201 Lowell Street Wilmington, MA 01887
3	BLM Applied Mechanics Consultants ATTN: A. Boresi R. Miller H. Langhaar 3310 Willett Drive Laramie, WY 82070
1	Martin Marietta Corporation ATTN: J.I. Bacile Orlando, FL 32805
1	H.P. White Laboratory 3114 Scarboro Road Street, MD 21154
1	CALSPAN Corporation ATTN: E. Fisher P.O. Box 400 Buffalo, NY 14225
1	FMC Corporation Ordnance Engineering Division San Jose, CA 95114
1	Kaman-Tempo ATTN: E. Bryant 715 Shamrock Road Bel Air, MD 21014
2	General Electric Armament and Electrical Systems ATTN: D.A. Graham M.J. Bulman Lakeside Avenue Burlington, VT 05402
1	Olin Corporation Badger Army Ammunition Plant ATTN: R.J. Thiede Baraboo, WI 53913
1	S&D Dynamics, Inc. ATTN: M. Soifer 755 New York Avenue Huntington, NY 11743
1	Southwest Research Institute ATTN: P.A. Cox 8500 Culebra Road San Antonio, TX 78228
1	Southwest Research Institute ATTN: T. Jeter 8500 Culebra Road San Antonio, TX 78228
1	University of Dayton Research Institute ATTN: S.J. Bless Dayton, OH 45469
1	University of Delaware Department of Mechanical Engineering ATTN: H. Kingsbury Newark, DE 19711
6	University of Illinois College of Engineering ATTN: A. Zak (2) D. C. Drucker Urbana, IL 61801
1	ASD (ENFTV, Martin Lentz) Wright-Patterson AFB OH 45433

DISTRIBUTION LIST

No. of Copies	Organization
2	University of Iowa College of Engineering ATTN: R. Benedict E.J. Haug Iowa City, IA 52240
1	Rutgers University Dept. of Mechanical and Aerospace Engineering ATTN: T. W. Lee New Brunswick, NJ 08903
1	University of Wisconsin Mechanical Engineering Depart ATTN: S.M. Wu Madison, WI 53706
1	University of Wisconsin Mathematics Research Center 610 Walnut Street ATTN: B. Noble Madison, WI 53706
1	AFFDL/FB (J. Halpin) Wright-Patterson AFB OH 45433
3	Honeywell, Inc. Government and Aerospace Products Division ATTN: G. Johnson J. Blackburn R. Simpson 600 Second Street, NE Hopkins, MN 55343
4	Director Los Alamos Scientific Lab ATTN: Tech Lib J. Taylor R. Karpp U. F. Kocks P.O. Box 1663 Los Alamos, NM 87544
4	Director Sandia National Laboratories ATTN: L. Davison P. Chen L. Bertholf W. Herrmann Albuquerque, NM 87115
4	SRI International ATTN: D. Curran L. Seaman Y. Gupta G.R. Abrahamson 333 Ravenswood Avenue Menlo Park, CA 94025
5	Brown University Division of Engineering ATTN: R. Clifton H. Kolsky A. Pipkin P. Symonds J. Martin Providence, RI 02912
3	California Institute of Technology Division of Engineering and Applied Science ATTN: J. Miklowitz E. Sternberg J. Knowles Pasadena, CA 91102
1	University of California at Los Angeles Department of Mechanics ATTN: W. Goldsmith Los Angeles, CA 90024
1	Drexel Institute of Technology Wave Propagation Research Center ATTN: P.C. Chou 32nd and Chestnut Streets Philadelphia, PA 19104

DISTRIBUTION LIST

No. of Copies	Organization
1	Harvard University Division of Engineering and Applied Physics ATTN: G. Carrier Cambridge, MA 02138
1	Iowa State University Department of Engineering Science and Mechanics ATTN: C.P. Burger Ames, IA 50010
2	Iowa State University Engineering Research Lab ATTN: G. Nariboli A. Sedov Ames, IA 50010
4	The Johns Hopkins University ATTN: J. Bell R. Green R. Pond, Sr. C. Truesdell 34th and Charles Streets Baltimore, MD 21218
1	Commander US Army Missile Command ATTN: DRCPM-HD Redstone Arsenal, AL 35898
4	Massachusetts Institute of Technology ATTN: R. Probstein A.S. Argon F. McClintock K.J. Bathe 77 Massachusetts Avenue Cambridge, MA 02139
1	New Mexico Institute of Mining and Technology Terra Group Socorro, NM 87801
1	Rensselaer Polytechnic Inst Department of Mechanical Engineering ATTN: E. Krempl Troy, NY 12181
2	Southwest Research Institute Department of Mechanical Sciences ATTN: U. Lindholm W. Baker 8500 Culebra Road San Antonio, TX 78228
2	University of Delaware Department of Mechanical Engineering ATTN: J. Vinson M. Taya Newark, DE 19711
3	University of Florida Department of Engineering Science and Mechanics ATTN: C. Sciammarilla L. Malvern E. Walsh Gainesville, FL 32601
2	University of Illinois at Chicago Circle College of Engineering Dept. of Materials Engineering ATTN: A. Schultz T.C.T. Ting P.O. Box 4348 Chicago, IL 60680
2	University of Minnesota Department of Engineering Mechanics ATTN: R. Fosdick J. Erickson Minneapolis, MN 55455

DISTRIBUTION LIST

No. of Copies	Organization
1	Yale University Department of Engineering and Applied Science ATTN: A. Phillips New Haven, CT 06520
2	Washington State University Department of Physics ATTN: G. E. Duvall, R. Fowles Pullman, WA 99163
1	AFELM, The Rand Corporation ATTN: Library-D 1700 Main Street Santa Monica, CA 90406

Aberdeen Proving Ground

Dir, USAMSAA
ATTN: DRXSY-D
DRXSY-MP, H. Cohen
DRXSY-G, E. Christman
DRXSY-OSD, H. Burke
DRXSY-G, R. C. Conroy
DRXSY-LM, J.C.C. Fine

Dir, USAHEL
ATTN: DRXHE, A.H. Eckles, III

Cdr, USATECOM
ATTN: DRSTE-TO-F
DRSTE-CE

Cdr, CRDC, AMCCOM
ATTN: DRSMC-CLB-PA
DRSMC-CL
DRSMC-CLB
DRSMC-CLD
DRSMC-CLY
DRSMC-CLN
DRSMC-CLN-D, L. Shaff
DRSMC-CLN-D, F. Dagostin
DRSMC-CLN-D, C. Hughes
DRSMC-CLN, J. McKivrigan
DRSMC-CLJ-L

USER EVALUATION OF REPORT

Please take a few minutes to answer the questions below; tear out this sheet, fold as indicated, staple or tape closed, and place in the mail. Your comments will provide us with information for improving future reports.

1. BRL Report Number _____

2. Does this report satisfy a need? (Comment on purpose, related project, or other area of interest for which report will be used.)

_____

_____

_____

3. How, specifically, is the report being used? (Information source, design data or procedure, management procedure, source of ideas, etc.) _____

_____

_____

4. Has the information in this report led to any quantitative savings as far as man-hours/contract dollars saved, operating costs avoided, efficiencies achieved, etc.? If so, please elaborate.

_____

_____

5. General Comments (Indicate what you think should be changed to make this report and future reports of this type more responsive to your needs, more usable, improve readability, etc.) _____

_____

_____

_____

6. If you would like to be contacted by the personnel who prepared this report to raise specific questions or discuss the topic, please fill in the following information.

Name: _____

Telephone Number: _____

Organization Address: _____

_____

_____

FOLD HERE

Director
US Army Ballistic Research Laboratory
ATTN: DRSMC-BLA-S (A)
Aberdeen Proving Ground, MD 21005

NO POSTAGE
NECESSARY
IF MAILED
IN THE
UNITED STATES

OFFICIAL BUSINESS
PENALTY FOR PRIVATE USE, $300

BUSINESS REPLY MAIL
FIRST CLASS PERMIT NO 12062 WASHINGTON, DC
POSTAGE WILL BE PAID BY DEPARTMENT OF THE ARMY

Director
US Army Ballistic Research Laboratory
ATTN: DRSMC-BLA-S (A)
Aberdeen Proving Ground, MD 21005

FOLD HERE